ANALYSIS AND SIMULATION OF DIRECT TORQUE CONTROLLED INDUCTION MOTOR DRIVE

A THESIS SUBMITTED IN PARTIAL FULFILMENT OF THE

REQUIREMENTS FOR THE DEGREE OF

Bachelor of Technology

In

ELECTRICAL ENGINEERING

By

AMRIT SAHOO (110EE0225)

ARPIT MOHANTY (110EE0208)

Under the guidance and supervision of

Prof. Gopalakrishna Srungavarapu

Dept. of Electrical Engineering

NIT, Rourkela

Dept. of Electrical Engineering
National Institute of Technology Rourkela,
Rourkela – 769008, India
May 2014

Department of Electrical Engineering
National Institute of Technology
Rourkela – 769008
May 2014

CERTIFICATE

This is to certify that the thesis titled, **"Analysis and Simulation of Direct Torque Controlled Induction Motor Drive"** submitted by **AMRIT SAHOO (110EE0225)** and **ARPIT MOHANTY (110EE0208)** in partial fulfillment of the requirements for the award of Bachelor of Technology Degree in Electrical Engineering at the National Institute of Technology, Rourkela is a genuine work carried out by them under my supervision and guidance. To the best of my knowledge, the material embodied in the thesis has not been submitted to any other university/institute for the award of any degree or diploma.

Place:
Date:

Dr. Gopalakrishna Srungavarapu
Assistant Professor
Department of Electrical Engineering
National Institute of Technology, Rourkela

To

God and our Parents

ACKNOWLEDGMENT

We would like to express gratitude to NIT, Rourkela for providing its resources and sanctioning me to work in such a stimulating environment. We will take this chance to offer our special gratitude to our final year project supervisor ***Prof. Goplalakrishna Srungavarapu*** for his able guidance and judicious help during our project work in spite of his busy schedule. This project would not have been potential without his help and valuable time. We would also like to acknowledge all the staff members of the department of Electrical Engineering who have been very cooperative with us.

AMRIT SAHOO (110EE0225)
APRIT MOHANTY (110EE0208)
Dept. of Electrical Engineering
National Institute of Technology
Rourkela - 769008

ABSTRACT

Induction motors were earlier used mainly in uses requiring constant speed because orthodox procedures of their speed control have either been expensive or exceedingly wasteful. Variable speed applications have been dominated by dc drives. The main drawback of dc motors is the presence of commutator and brushes, hence requiring regular maintenance and making them unsuitable for explosive environments. While induction motors are rugged, cheaper, lighter, smaller, and more efficient. Convenience of transistors, IGBTs, and GTO have allowed the advance of variable speed induction motor drives. Such recent trends in speed control methods of induction motor have led to their enormous use in all electric drives.

Numerous methods of speed control of an induction motor, e.g. pole changing, frequency variation, variable rotor resistance, variable stator voltage, constant V/f control, slip recovery method, field oriented control etc., are being employed presently. These methods can be classified into two types- scalar control and vector control. In scalar control load speed and position are not measured as in a servo system, while in vector control either the speed or the position or both are controlled as in a servo system. Among the scalar control, closed loop constant V/f speed control method is the most commonly used. In this method, the V/f ratio is preserved constant which in turn upholds magnetizing flux constant, hence maximum electromagnetic torque remains unchanged. Hence, the procedure absolutely exploits the motor.

The vector control study of an induction motor countenances the decoupled analysis. In this control torque and flux components are independently controlled (just as in dc motor). This simplifies the analysis compared to the per phase equivalent circuit. The major disadvantage of flux vector control is the required insertion of the pulse encoder. The other disadvantage is that torque is indirectly controlled rather than directly. Lastly, a delay in signal of input references and resultant stator voltage vector is introduced because of presence of the PWM modulator. The last two factors prevent the eventual capability of vector control to attain high express flux and torque control.

Direct torque control (DTC) of an induction motor fed by a voltage source inverter is a modest scheme that does not need lengthy computation time and can be implemented without pulse encoders and is unresponsive to parameter variations. The objective is to control efficiently torque and flux. This procedure estimates motor flux and torque by sampling and analyzing motor terminal voltages and currents. A voltage vector is nominated to have flux and torque errors within boundaries, built on estimations of flux position and amount of instantaneous errors in torque and stator flux. This method made the motor control more accurate and fast, highly dynamic speed response and simple to control. The reference value can be evaluated using the flux and torque estimated and motor parameters. The effectiveness of the Direct Torque Control scheme was verified by simulation using **MATLAB/SIMULINK®.**

CONTENTS

LIST OF FIGURES

LIST OF TABLES

CHAPTER 1

INTRODUCTION

1.1. Overview

1.2. Historical review

1.3. Features of Direct Torque Control

1.4. Overview of the thesis

1.1. Overview

Motion control is required everywhere, be it domestic application or industry. The systems that are engaged for this purpose are called drives. Such a system, if uses electric motors for control is known as an electrical drive. In electrical drives, various sensors and control algorithms are employed to control the speed of the motor using suitable speed control methods. The basic block diagram of an electrical drive is shown below:

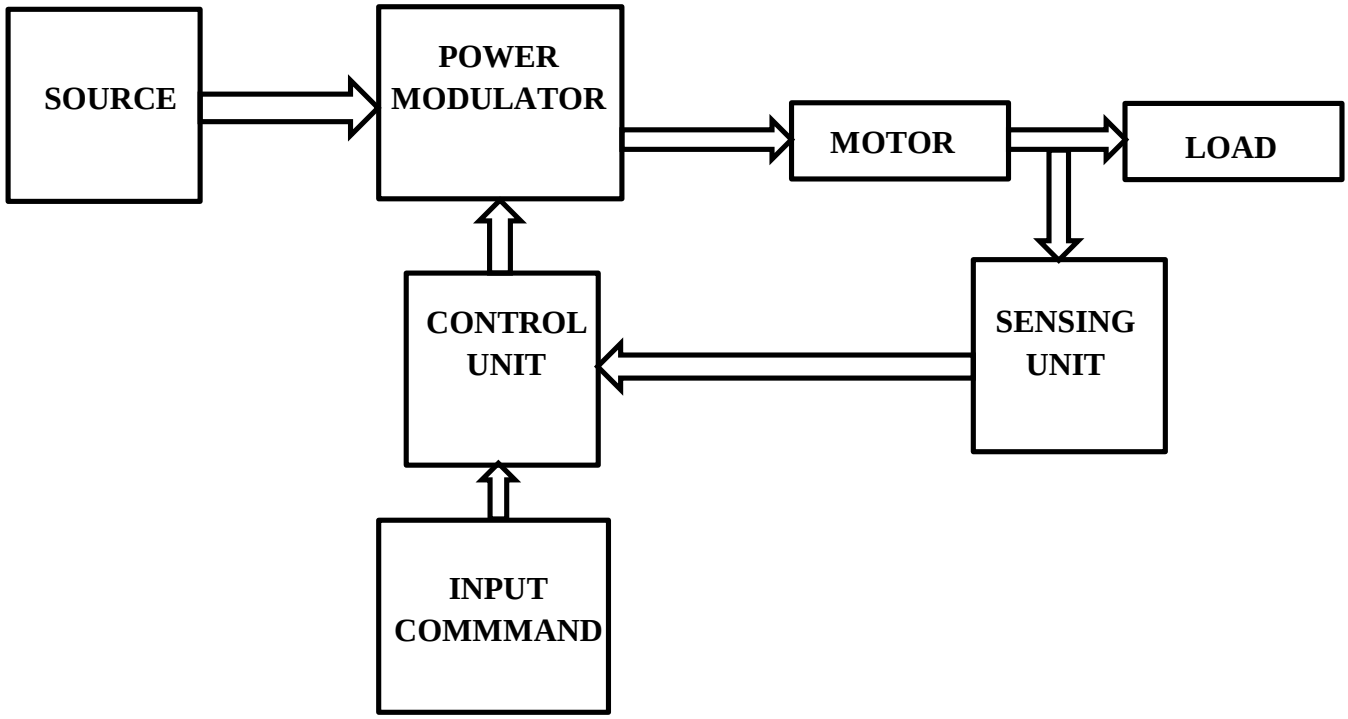

Figure 1.1: Block diagram of an electric drive

1.2. HISTORICAL REVIEW:

DC motors were ruling the variable speed actuators prior to invention of µcontrollers and high switching frequency semiconductor devices. Presently frequency, phase and magnitude of supply to AC motor are easily being reformed by the application of fast switching power converters controlled by µcontrollers. Hence variable speed drives are nowadays equipped with induction motors.

The major benefit is that in induction motors stationary and rotating parts are electrically isolated. So, there is no need of any mechanical commutator, hence enabling IMs to be damage-proof motors. Induction motors possess low weight and inertia, high efficiency and a high overload capability. Hence, they are cheaper and more robust. Supplying the induction motor with 3-ϕ voltages of variable frequency and magnitude is the most operative way of manufacturing substantially variable speed induction motor drive. Rotor speed is proportionate to speed of rotating magnetic field formed in air gap due to 3-ϕ currents in stator, hence variable frequency supply is essential. At lower frequencies the impedances of motor decreases, hence the motor current increases substantially. In order to decrease the current at lower frequencies, voltages with varying magnitudes

are essential. Prior to introduction of power electronics, voltage at the motor windings was varied by swapping the winding connections from delta to star, thus enabling in partial speed control of induction motor.

Definite distinct speeds of induction motors can be attained from motors made of stator windings more than three. This changes the number of pole pairs of motor. Such motors are costlier as more than three contacts to the motor are necessary.

There has been evolution of many controllers for AC motors:

1.1.1. Flux Vector Control

By applying this, control based on flux vector rebuilds a major merit of dc drive. When we consider this situation, we attain an electronic orientation of the field. Founded on comparative evaluation of identified stator field vector to response of rotor angular position and speed, this procedure evaluates and controls spatial angular position of rotor flux. µprocessor procedures are employed to analytically model electric features of the motor so as to empower fast data processing. Torque control is indirect, but, good torque response is achieved. Jazzed up speed and torque precision can be attained by addition of the pulse encoder. This addition of pulse encoder is major drawback of the procedure. Torque is controlled indirectly, rather than directly. This also proves to be a major drawback. Another drawback is the delay in signal of input references and resultant stator voltage vector is introduced because of presence of the PWM modulator.

1.1.2. Direct Torque Control

Hysteresis controller is employed to regulate both flux and torque. An optimal switching logic is employed as a replacement for PWM modulator. Thus, delays related to PWM modulator stage. Direct flux control and fast responsiveness are the unique benefits related with dc drive of direct torque control. Torque response of the procedure proves to be improved than that obtainable with either dc or flux vector control. Requirement of pulse encoder is eliminated in order to achieve reasonable speed accuracy (typically 0.1%–0.3% or 10% of motor slip).

1.3. FEATURES OF DIRECT TORQUE CONTROL:

DTC main features are as follows:

- Direct control of flux and torque.
- Approximately sinusoidal stator fluxes and stator currents.
- High dynamic performance even at stand still.

The main advantages of DTC are:

- Absence of co-ordinate transforms.
- Absence of voltage modulator block and other controllers, e.g. PID for motor flux and torque.
- Minimal torque response time, even better than the vector controllers.

The disadvantages of DTC are:

- Problems during starting.
- Necessity of torque and flux predictors, implying the consequent parameters identification.
- Intrinsic torque and stator flux ripple.

1.4. OVERVIEW OF THE THESIS:

Chapter 2 gives a review of the analysis of the three phase induction motor. It contains the equivalent circuit of the motor. From the equivalent circuit the necessary equations were derived.

Chapter 3 gives a review of the induction motor modeling, and of the field-oriented control methods and their limitations. A SIMULINK model is developed for the induction machine model and simulated for three phasors to two phase transformation of induction machine model.

Chapter 4 covers the fundamentals of the principle of DTC of induction motors and methods to deal with DTC limitations on flux estimation accuracy are discussed in detail. A SIMULINK model and MATLAB iterative technique programed are used to simulate the conventional DTC of induction motor.

Chapter 5 gives the summary, conclusions and directions for future work.

CHAPTER 2

ANALYSIS OF THREE PHASE INDUCTION MOTOR

2.1. Equivalent circuit analysis

2.2. Torque-speed curve

2.1. Equivalent circuit analysis

Based on the construction of the rotor, a 3-ϕ induction motor can be categorized into two types:

I. Squirrel Cage Induction Motor

II. Wound Rotor or Slip Ring Induction Motor

Three phase balance distributed windings, each phase physically placed 120^0 apart from each other are placed in the stator of both types of motors. When 3-ϕ currents flow through windings of stator, a rotating magnetic field is generated in the air gap.

Assuming the three phases to be balanced, the analysis of a 3-ϕ induction motor can be made by analyzing the equivalent circuit of only one of the phases. We now derive the per-phase equivalent circuit of an IM. The synchronously rotating air gap flux wave generates a counter voltage $\mathbf{V_m}$. This is converted to slip voltage, $\mathbf{V_r}'$, i.e.

$$\mathbf{V_r}' = \mathbf{nsV_m} \tag{2.1}$$

in rotor phase, where n = rotor-to stator-turns ratio and s = per unit slip. Slip s is given by

$$\mathbf{s} = \frac{\omega_s - \omega_m}{\omega_s} \tag{2.2}$$

where, ω_m and ω_s are rotor and synchronous speeds, respectively.

The stator terminal voltage $\mathbf{V_s}$ differs from voltage $\mathbf{V_m}$ by reduction in stator resistance R_s and stator leakage inductance L_{ls}. Excitation current $\mathbf{I_0}$ consists of two components: core-loss component I_c and magnetizing component I_m.

The rotor induced voltage $\mathbf{V_r}'$ causes rotor current Ir' at slip frequency ω_{sl}. Current is limited by rotor resistance R_r' and rotor leakage inductance L_{lr}'. Stator current I_s is addition of excitation component I_o and rotor-reflected current I_r.

The rotor-reflected current I_r is given by:

$$I_r = nI_r' = \frac{n^2 s V_m}{R_r' + j\omega_{sl} L_{lr}'} = \frac{V_m}{\frac{R_r}{s} + j\omega_s L_{lr}} \tag{2.3}$$

where parameters $R_r = R_r'/n^2$ and $L_{lr} = L_{lr}'/n^2$ are referred to the stator.

The speed of the rotating air gap flux produced can be expressed as:

$$\omega_s = \frac{120 * f}{P} \text{ rpm} \tag{2.4}$$

where f and P are supply frequency and number of poles, respectively.

The per phase equivalent circuit of an induction motor is shown below:

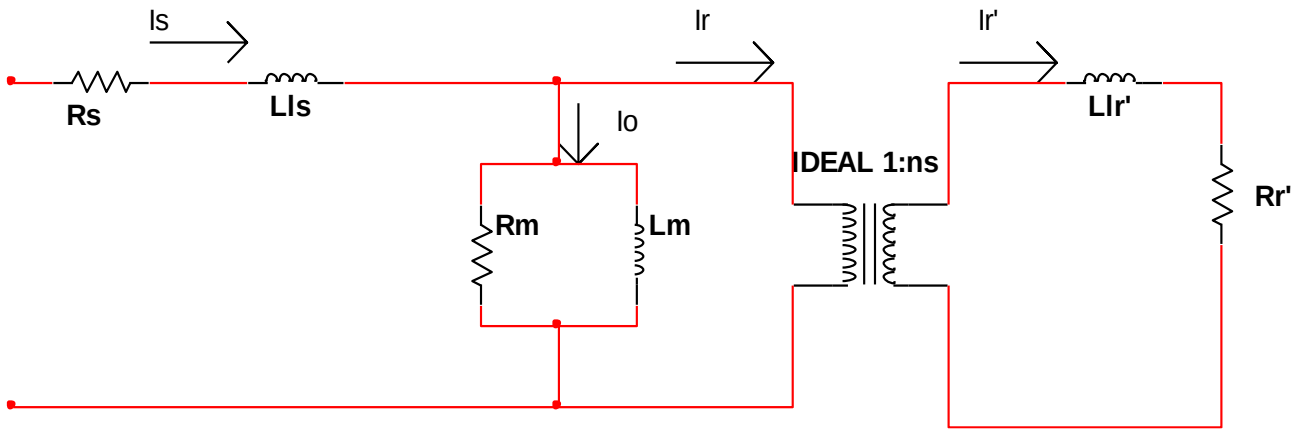

Figure 2.1.: Equivalent circuit transformer coupling

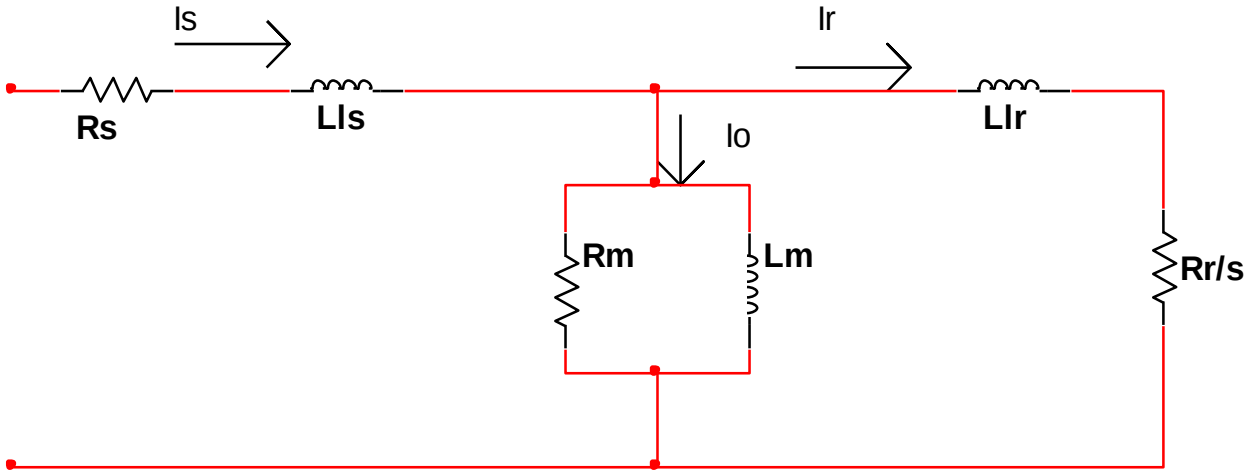

Figure 2.2: Per phase equivalent circuit w.r.t stator

Stator impedance drop is generally negligible compared to terminal voltage V_s, the core loss resistor R_m has been dropped and the magnetizing inductance L_m is shifted at the input. The equivalent circuit is shortened to as shown below:

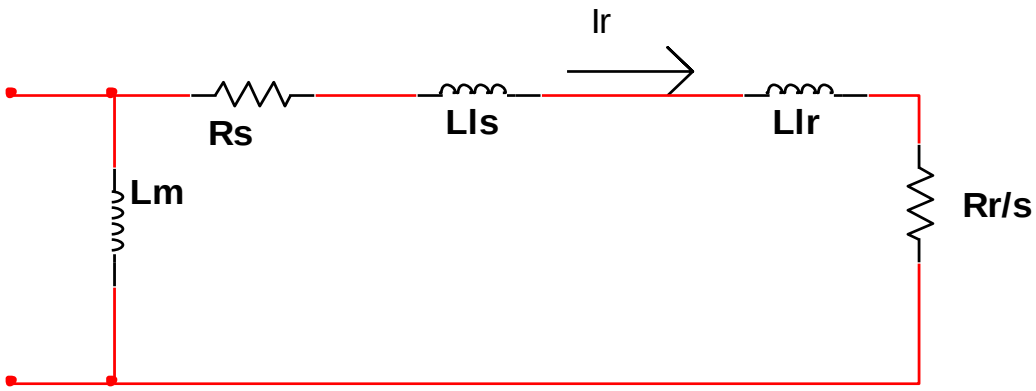

Figure 2.3: Approximate per phase equivalent circuit

The magnitude of stator raised rotor current, I_r is given by:

$$I_r = \frac{V_s}{\sqrt{\left(R_s + \frac{R_r}{s}\right)^2 + (X_s + X_r)^2}} \quad (2.5)$$

Power transferred to rotor (or air-gap power), P_g is given by:

$$P_g = 3I_r^2 \frac{R_r}{s} \quad (2.6)$$

Rotor copper loss, P_{Cu} is given by:

$$P_{Cu} = 3\ I_r^2\ R_r \quad (2.7)$$

Total electrical power converted into mechanical power is:

$$P_m = P_g - P_{Cu} = 3\ I_r^2\ R_r \left(\frac{1 - s}{s}\right) \quad (2.8)$$

Electromagnetic torque developed by motor is:

$$T = P_m / \omega_m \quad (2.9)$$

Thus,

$$T = \frac{3}{\omega_s} \frac{I_r^2\ R_r}{s} \quad (2.10)$$

Substituting the value of I_r into the above equation, we get,

$$T = \frac{3\ V_s^2}{\omega_s\left[\left(R_s + \frac{R_r}{s}\right)^2 + (X_s + X_r)^2\right]} \frac{R_r}{s} \quad (2.11)$$

Differentiating T with respect to s and equating to zero gives the slip for maximum torque, i.e.

$$s_m = \pm \frac{R_r}{\sqrt{R_s^2 + (X_s + X_r)^2}} \quad (2.12)$$

Substituting s_m in T gives the value of maximum torque, thus the maximum electromagnetic torque is given by:

$$T_{max} = \frac{3}{2} \frac{V_o^2}{\omega_s\left[R_s \pm \sqrt{R_s^2 + (X_s + X_r)^2}\right]} \quad (2.13)$$

2.2. Torque-Speed Curve

The developed electromagnetic torque can be calculated as a function a slip from equation 2.11. The torque-speed curve is plotted by the use of the equation and a MATLAB program which is presented in the appendix. The zones are defined as plugging (1<s<2), motoring (0<s<1) and regenerating (s<0).

In the normal motoring region T = 0 @ s = 0. T increases as s increases in a quasi-linear curve until maximum torque is reached. Beyond maximum torque, T decreases with increase in s.

In the plugging region the rotor rotates in the opposite direction to that of the air gap flux. This condition may arise if stator supply phase sequence is reversed when rotor is moving or an overhauling load drives the rotor in opposite direction.

In the regenerating region the rotor moves at supersynchronous speed in the same direction as that of the air gap flux. The slip becomes negative. The negative resistance R_r/s generates energy and supplies it to source. So the motor acts as generator.

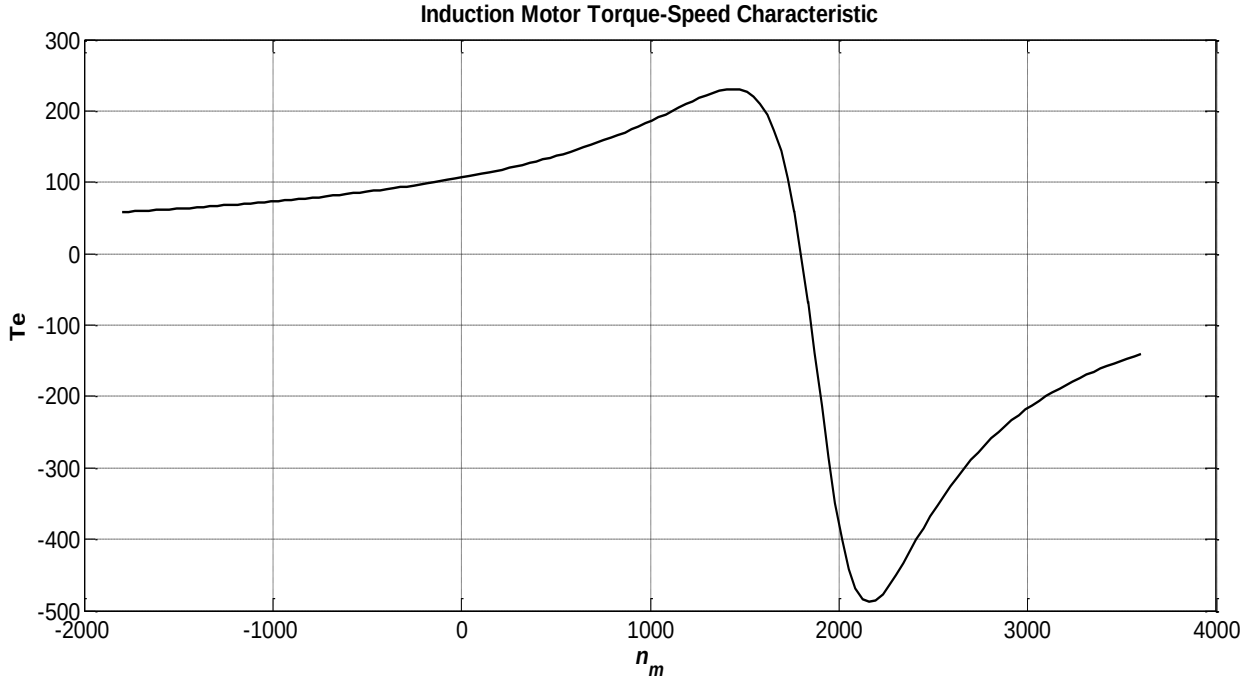

Figure 2.4: Torque-speed curve of induction motor

CHAPTER 3

TRANSIENTS DURING STARTING OF 3-ϕ INDUCTION MOTOR

3.1 Transient analysis using SIMULINK Model

3.2 Interim Conclusions

3.1. Transients during Starting Of 3-Φ Induction Motor

We design a MATLAB SIMULINK 3-ϕ induction motor prototype and then plot the rotor and stator currents, speed, electromagnetic torque and the Torque-Speed characteristics were observed with different values of rotor and stator resistances and impedances.

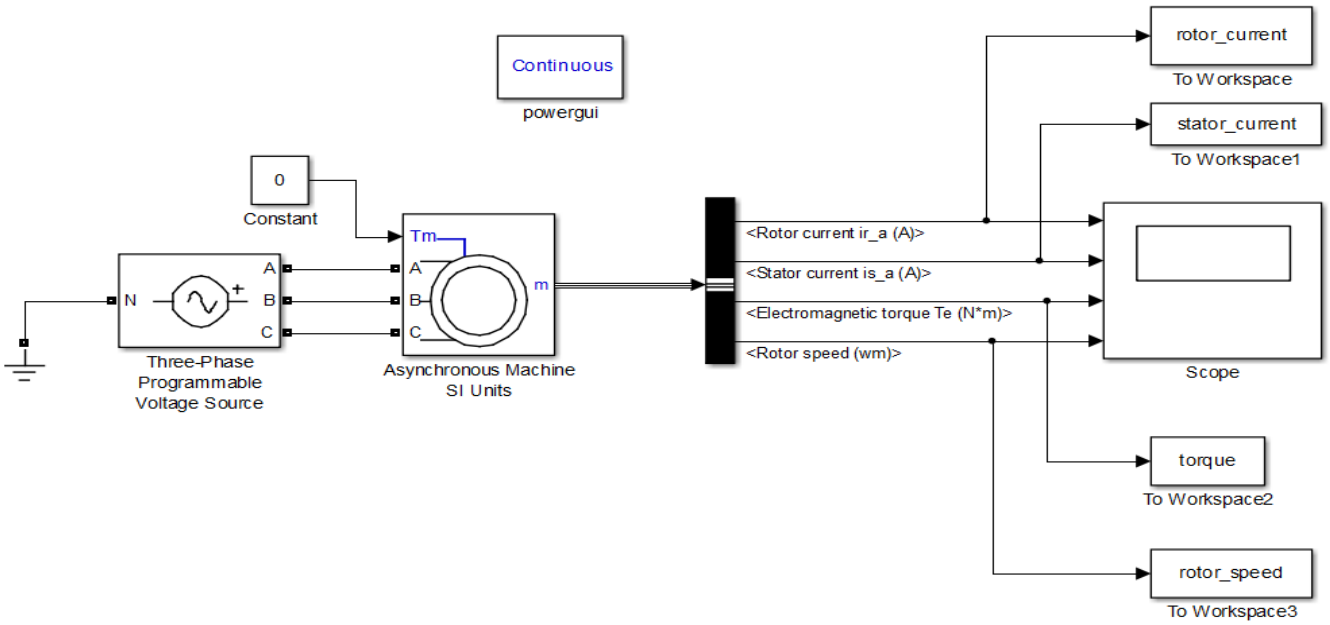

Figure 3.1: SIMULINK Model of a 3-ϕ IM

The different machine details followed by their corresponding outcomes are shown in this chapter.

It should be noted that all the simulations were made for Zero Load Torque. However, the inertia and friction were taken into consideration.

3.1.1. Low Stator Inductance (~0.05mH)

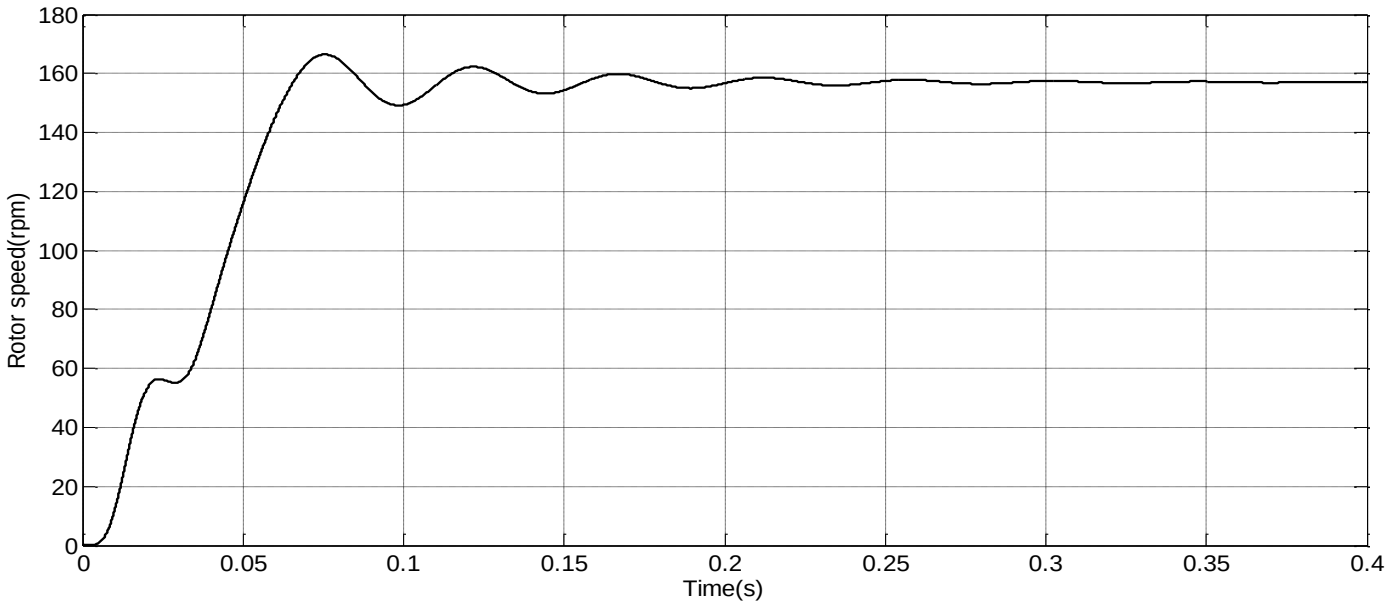

Figure 3.2: Rotor speed vs Time

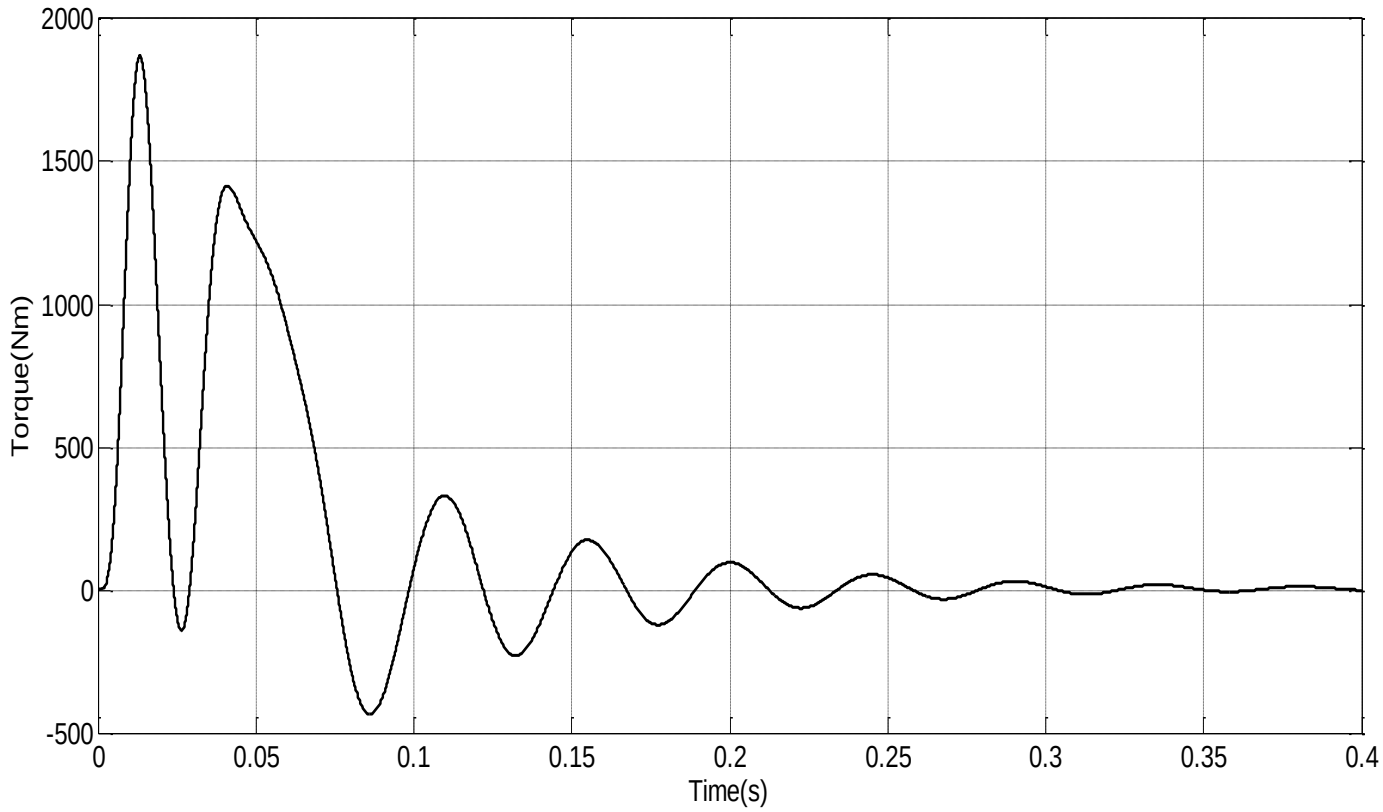

Figure 3.3: Torque vs Time

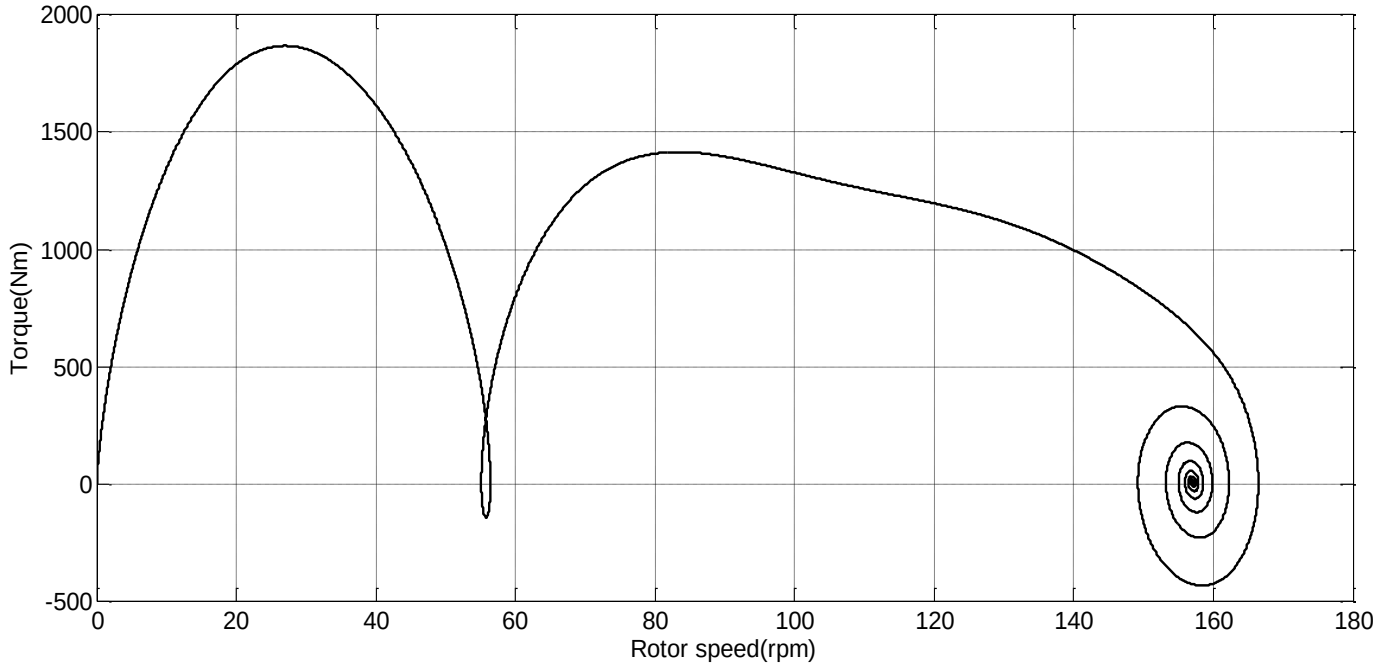

Figure 3.4: Torque vs rotor speed

3.1.2. Medium stator inductance (~0.7mH)

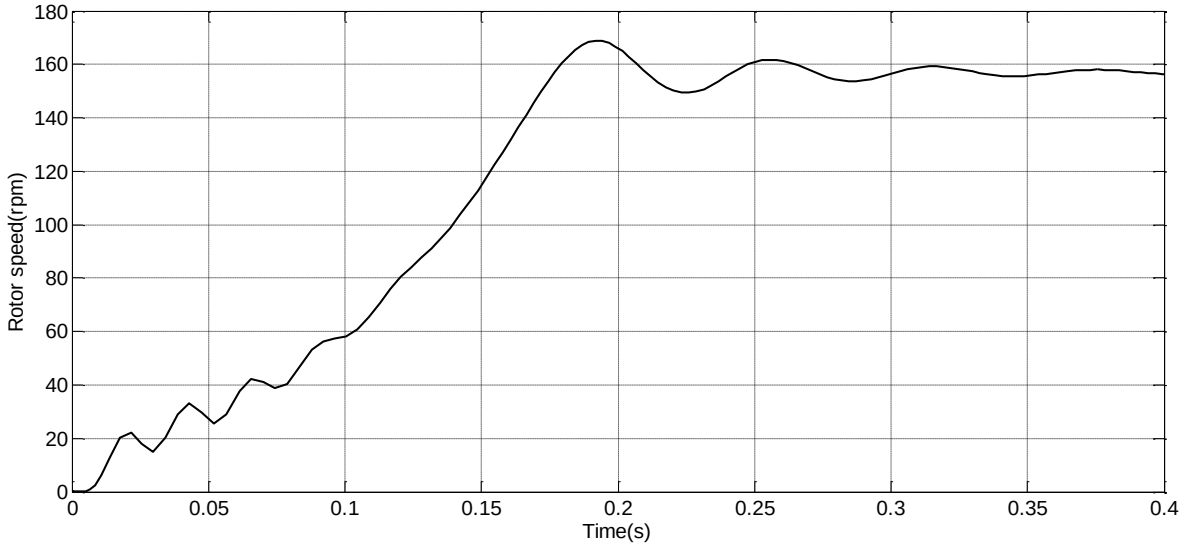

Figure 3.5: Rotor speed vs time

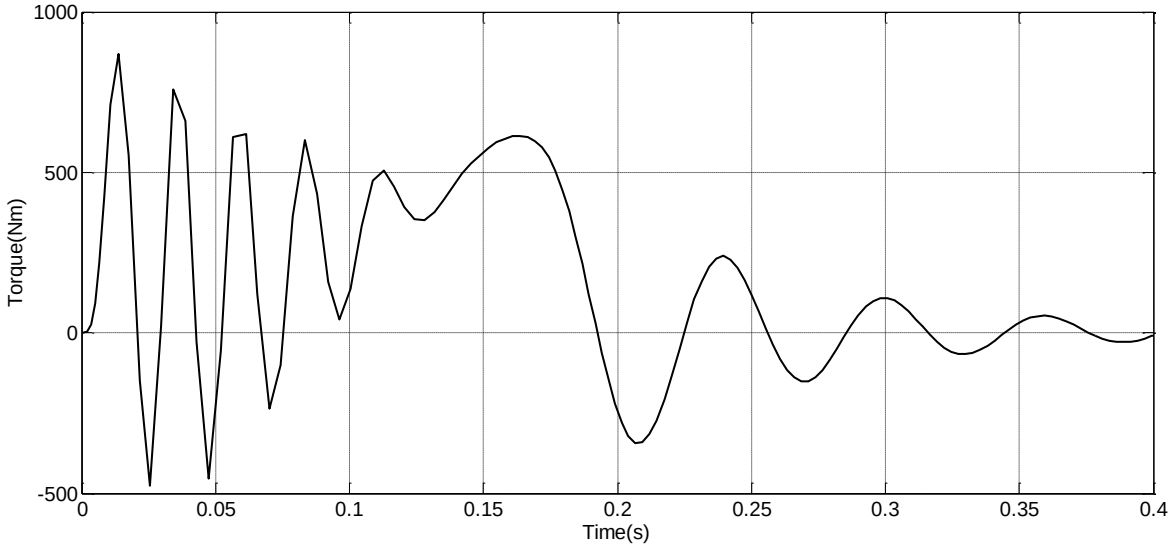

Figure 3.6: Torque vs time

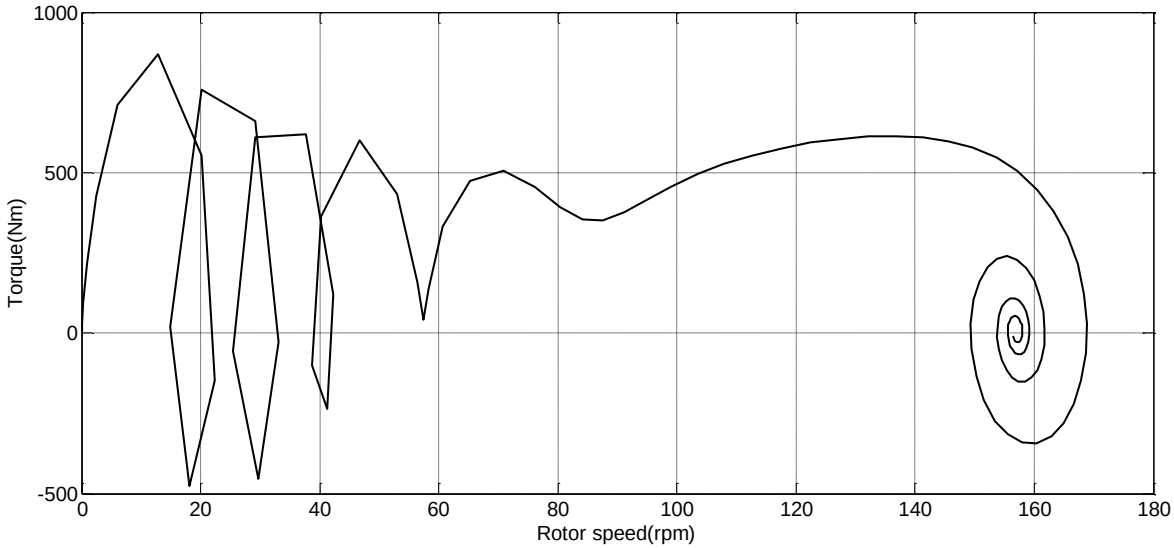

Figure 3.7: Rotor speed vs torque

3.1.3. High stator inductance (~2mH)

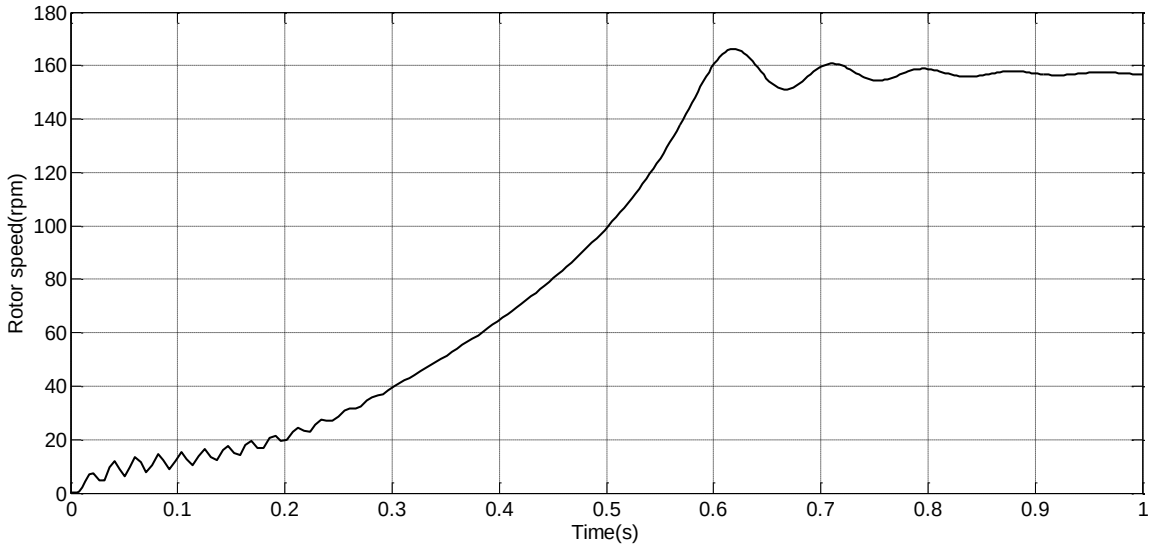

Figure 3.8: Rotor speed vs time

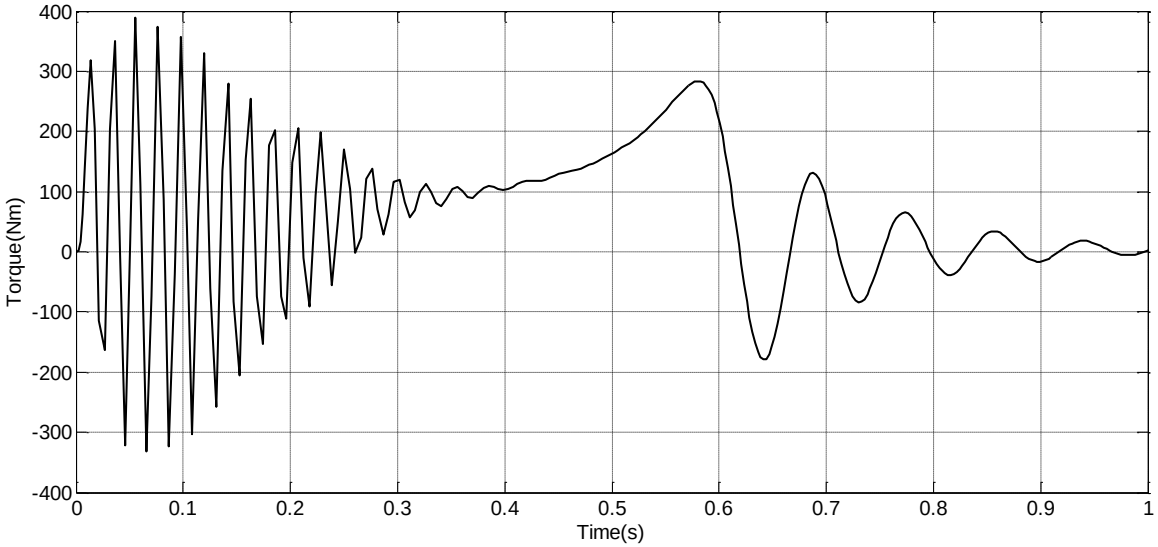

Figure 3.9: Torque vs time

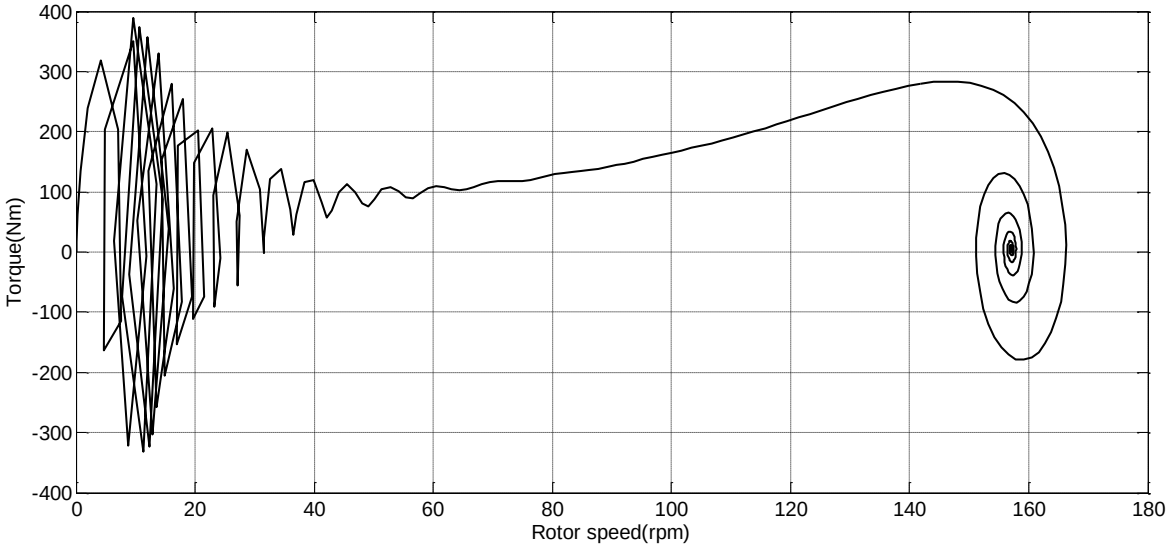

Figure 3.10: Torque vs Rotor speed

3.2. Interim Conclusions

We draw the following observations, based on above results:

i. The transients are directly proportionate to both rotor and stator motor inductance. The transients decayed down slowly on increasing the motor inductance (either rotor or stator), i.e. steady state values were achieved slowly. The motor was bumpy while starting.

ii. The starting of the motor was less bumpy when the rotor resistance was more. Although the steady state time remain unchanged, the oscillations during transients decreased. Also the motor attained peak torque at lesser speed.

iii. The starting of the motor was bumpier when the stator resistance was more. The steady state values also reached slowly. Thus the stator resistance must be kept as low as possible.

CHAPTER 4

ANALYSIS OF VARIOUS METHODS FOR SPEED CONTROL OF IM

4.1 Introduction

4.2 Variable rotor resistance

4.2 Variable stator voltage

4.3 Constant V/f method

4.1. Introduction

The various methods of speed control of 3-ϕ Induction motor are as under:

1. Pole Changing
2. Variable Supply Voltage Control
3. Variable rotor resistance control
4. Variable Supply Frequency Control
5. Constant V/f control
6. Slip recovery
7. Vector Control

However, we shall not be analyzing the pole changing and the variable supply frequency methods as these are very rarely used. This chapter deals with the basic theory behind the several methods of speed control. Hereafter, they are discussed one after the other.

4.2. Variable Rotor Resistance

This method is applicable only to the wound rotor motor as external resistance can be added to it through the slip rings. A MATLAB code was developed to observe the variation in Torque-Speed characteristics of a 3-ϕ induction motor with variable rotor resistance. The MATLAB code is given in Appendix 1 and the output Torque-Speed characteristics are shown in Figure 4.1 below. The machine details used for the code execution are shown in Table 1 at the end of the chapter.

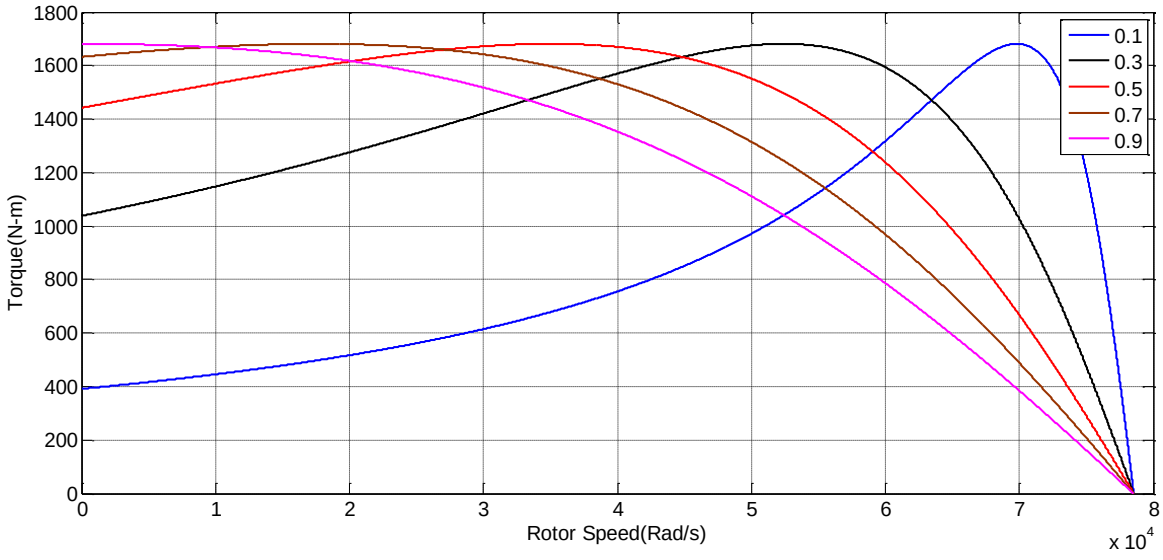

Figure 4.1: Torque-Speed characteristics of a 3-ϕ IM with Variable rotor resistance

External resistances can be connected in the rotor circuit during starting. This increases the starting torque (Equation 2.9 with s = 1) and reduces the starting current (Equation 2.3). By making use of appropriate value

of resistors, the maximum torque can be made to appear during starting. This can be used in applications requiring high starting torque. Once the motor is started, the external resistance can be cut out to obtain high torque throughout the accelerating range. As external resistances are connected, most of the I^2R loss is dissipated through them thus the rotor temperature rise during starting is limited.

4.3. Variable Stator Voltage

As can be seen from Equation 2.9, the torque developed by an induction motor varies as square of the voltage applied to its stator terminals. Thus by varying the applied voltage, the electromagnetic torque developed by the motor can be varied. This method is generally used for small squirrel-cage motors where cost is an important criterion and efficiency is not. However, this method has rather limited range of speed control.

A MATLAB code was developed to observe the variation in torque-speed characteristics of a 3-ϕ induction motor with variable stator voltage. The MATLAB code is given in Appendix 2 and the output Torque-Speed characteristics are shown in Figure 4.2 below. The machine details used for the code execution are shown in Table 1 at the end of the chapter.

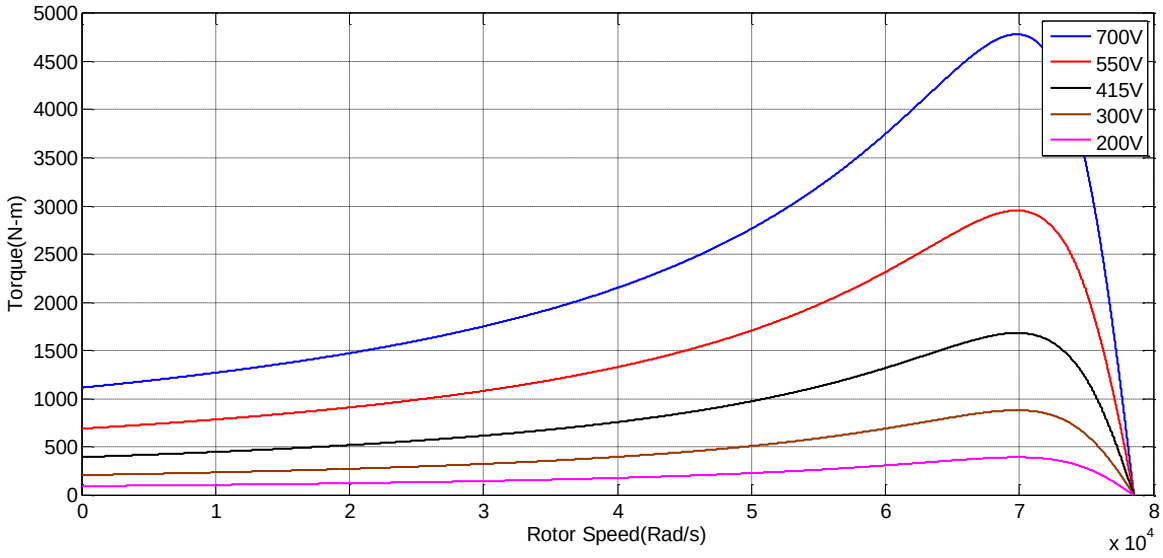

Figure 4.2: Torque-Speed characteristics of a 3-ϕ IM with Variable stator voltage

As the supply voltage is decreased, the value of maximum torque also decreases (Equation 2.11). However it still occurs at the same slip as earlier (Equation 2.10). Even the starting torque and the overall torque reduce (Equation 2.9). Thus the machine is highly underutilized. Thus this method of speed control has very limited applications.

4.4. Constant V/f Control

We vary the stator voltage in such a way that the flux remains constant by simultaneously varying the supply frequency in such a way that the ratio V/f remains constant. A MATLAB code was developed to observe the

variation in torque-speed characteristics of a 3-ϕ induction motor with constant V/f. The MATLAB code is given in Appendix 3 and the output Torque-Speed characteristics are shown in Figure 4.3 below. The machine details used for the code execution are shown in Table 1 at the end of the chapter.

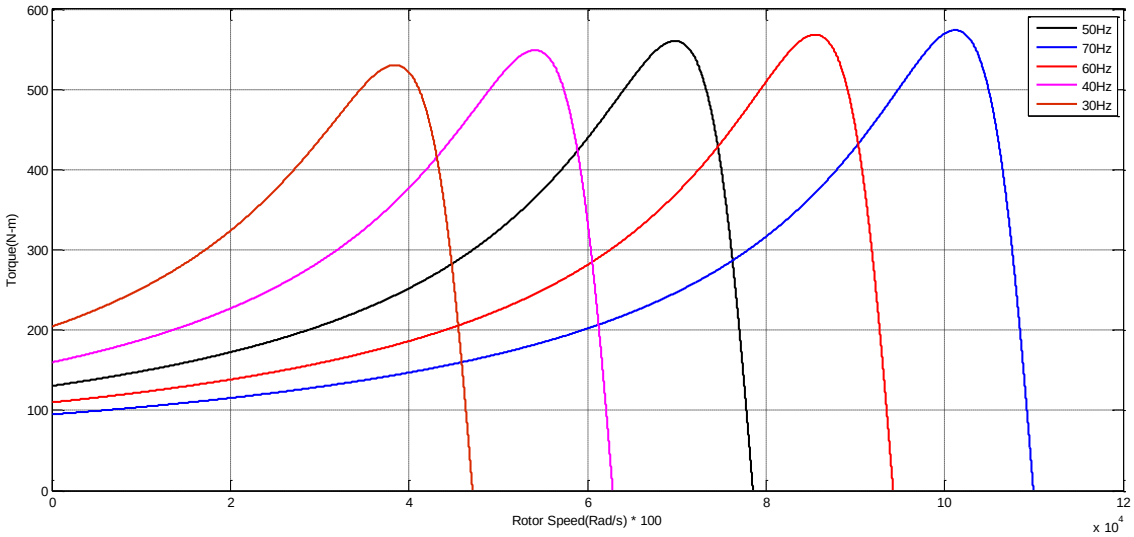

Figure 4.3: Torque-Speed characteristics of a 3-ϕ IM with constant V/f method

The AC supply is rectified and then applied to a PWM inverter to obtain a variable frequency, variable magnitude 3-ϕ AC supply. The magnetic field produced by the stator is one of the factor that directly governs the motor electromagnetic torque developed. We know the ratio of supplied voltage and frequency decides the flux produced by the stator. Hence, if we change both voltage and frequency by similar ratio, we can keep flux constant, which as we know will maintain the developed torque constant over the entire speed range. So this method is the most widely used method of speed control of an induction motor.

Table 4.1: Machine details used in MATLAB codes execution for variable rotor resistance, variable stator voltage and constant V/f control

RMS value of supply voltage (line-to-line)	415 Volts*
Number of poles	4
Stator resistance	0.075 ohm
Rotor resistance	0.1 ohm**
Frequency	50 Hz***
Stator leakage reactance at 50 Hz frequency	0.45 ohm
Rotor leakage reactance at 50 Hz frequency	0.45 ohm
V/f ratio (**ONLY FOR CONTANT V/f CONTROL)**	8.3

CHAPTER 5

INDUCTION MOTOR MODEL AND GENERALITIES

5.1 Equations of the Induction Motor Model

5.2 Space phasor Notation

5.3 Torque Expressions

5.4 SIMULINK model

5.5 Interim Conclusions

5.1. EQUATIONS OF THE INDUCTION MACHINE MODEL:

5.1.1. Introduction:

An element model of the machine subjected to control must be known so as to comprehend and outline vector controlled drives. Because of the way that each great control needs to face any conceivable change of the plant, it could be said that the element model of the machine could be simply a great rough guess of the genuine plant. Such a model might be acquired by method for either the space vector phasor hypothesis or two-pivot hypothesis of electrical machines. Notwithstanding the smallness and the straightforwardness of the space phasor hypothesis, both techniques are really close and both strategies will be clarified. For simplification, the induction motor considered will have the following assumptions:

- The two poles and the three phase windings are presumed perfectly Symmetrical
- The effects of slotting are ignored.
- It is supposed that the iron parts have unbounded permeability.
- The flux density wave that is existing in the air gap is assumed to be perfectly radial.
- The iron losses of the machine are neglected.
- The stator and the rotor windings are simplified as a single, multi-turn full pitch coil situated on the two sides of the air gap.

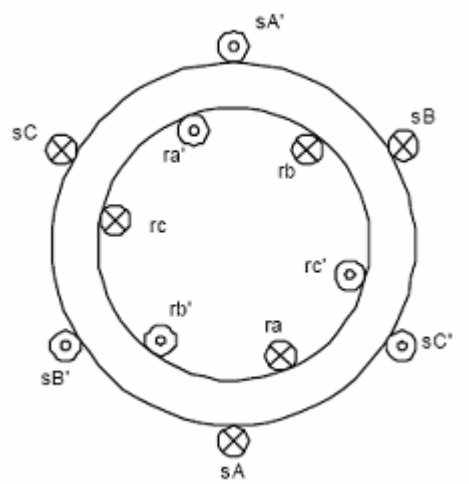

Figure 5.1: Cross section of elementary symmetrical three phase induction motor

5.1.2. Voltage equations

The stator voltages will be formulated in this section from the motor natural frame, which is the stationary reference frame fixed to the stator. In a similar way, the rotor voltages will be formulated to the rotating frame fixed to the rotor. In the stationary reference frame, the equations can be expressed as follows:

$$V_{sA} = R_s\, i_{sA}(t) + \frac{d\psi_{sA}(t)}{dt} \tag{5.1}$$

$$V_{sB} = R_s\, i_{sB}(t) + \frac{d\psi_{sB}(t)}{dt} \tag{5.2}$$

$$V_{sC} = R_s\, i_{sC}(t) + \frac{d\psi_{sC}(t)}{dt} \tag{5.3}$$

Similar expressions can be obtained for the rotor:

$$V_{rA} = R_r\, i_{rA}(t) + \frac{d\psi_{rA}(t)}{dt} \tag{5.4}$$

$$V_{rB} = R_r\, i_{rB}(t) + \frac{d\psi_{rB}(t)}{dt} \tag{5.5}$$

$$V_{rC} = R_r\, i_{rC}(t) + \frac{d\psi_{rC}(t)}{dt} \tag{5.6}$$

The immediate flux linkage value per phase in the stator is expressed as:

$$\psi_{sA} = \bar{L_s} i_{sA} + \overline{M_s} i_{sB} + \overline{M_s} i_{sC} + \overline{M_{sr}}\, i_{rA} \cos\theta_m + \overline{M_{sr}}\, i_{rB} \cos(\theta_m + 2\pi/3) + \overline{M_{sr}}\, i_{rC} \cos(\theta_m + 4\pi/3)$$

$$\psi_{sB} = \overline{M_s} i_{sA} + \bar{L_s} i_{sB} + \overline{M_s} i_{sC} + \overline{M_{sr}}\, i_{rA} \cos(\theta_m + 4\pi/3) + \overline{M_{sr}}\, i_{rB} \cos(\theta_m) + \overline{M_{sr}}\, i_{rC} \cos(\theta_m + 2\pi/3)$$

$$\psi_{sC} = \overline{M_s} i_{sA} + \overline{M_s} i_{sB} + \bar{L_s} i_{sC} + \overline{M_{sr}}\, i_{rA} \cos(\theta_m + 2\pi/3) + \overline{M_{sr}}\, i_{rB} \cos(\theta_m + 4\pi/3) + \overline{M_{sr}}\, i_{rC} \cos\theta_m \tag{5.7}$$

The immediate flux linkage value per phase in rotor is expressed as:

$$\psi_{rA} = \bar{L_r} i_{rA} + \overline{M_r} i_{rB} + \overline{M_r} i_{rC} + \overline{M_{sr}}\, i_{sA} \cos(-\theta_m) + \overline{M_{sr}}\, i_{sB} \cos(-\theta_m + 2\pi/3) + \overline{M_{sr}}\, i_{sC} \cos(-\theta_m + 4\pi/3)$$

$$\psi_{rB} = \overline{M_r} i_{rA} + \bar{L_r} i_{rB} + \overline{M_r} i_{rC} + \overline{M_{sr}}\, i_{sA} \cos(-\theta_m + 4\pi/3) + \overline{M_{sr}}\, i_{sB} \cos(-\theta_m) + \overline{M_{sr}}\, i_{sC} \cos(-\theta_m + 2\pi/3)$$

$$\psi_{rC} = \overline{M_r} i_{rA} + \overline{M_r} i_{rB} + \bar{L_r} i_{rC} + \overline{M_{sr}}\, i_{sA} \cos(-\theta_m + 2\pi/3) + \overline{M_{sr}}\, i_{sB} \cos(-\theta_m + 4\pi/3) + \overline{M_{sr}}\, i_{sC} \cos(-\theta_m) \tag{5.8}$$

In an analogous way, the immediate flux linkages in the rotor are expressed as:

$$\begin{bmatrix} V_{sA} \\ V_{sB} \\ V_{sC} \\ V_{rA} \\ V_{rB} \\ V_{rC} \end{bmatrix} = \begin{bmatrix} R_s + pL_s & pM_s & pM_s & pM_{sr}\cos\theta_m & pM_{sr}\cos\theta_{ml} & pM_{sr}\cos\theta_{ml} \\ pM_s & R_s + pL_s & pM_s & pM_{sr}\cos\theta_{ml} & pM_{sr}\cos\theta_m & pM_{sr}\cos\theta_{ml} \\ pM_s & pM_s & R_s + pL_s & pM_{sr}\cos\theta_{ml} & pM_{sr}\cos\theta_{ml} & pM_{sr}\cos\theta_m \\ pM_{sr}\cos\theta_m & pM_{sr}\cos\theta_{ml} & pM_{sr}\cos\theta_{ml} & R_r + pL_r & pM_r & pM_r \\ pM_{sr}\cos\theta_{ml} & pM_{sr}\cos\theta_m & pM_{sr}\cos\theta_{ml} & pM_r & R_r + pL_r & pM_r \\ pM_{sr}\cos\theta_{ml} & pM_{sr}\cos\theta_{ml} & pM_{sr}\cos\theta_m & pM_r & pM_r & R_r + pL_r \end{bmatrix} \begin{bmatrix} i_{sA} \\ i_{sB} \\ i_{sC} \\ i_{rA} \\ i_{rB} \\ i_{rC} \end{bmatrix} \tag{5.9}$$

5.1.3. Applying Park's transform:

In order to downsize the expressions for the induction motor equation, the voltages that are given in equation 5.1 to equation 5.6 and acquire definite coefficients for the differential equations, the Park's model is utilized. Physically, it is understood as reworking the 3 windings of the induction motor to merely 2 windings, because

it is shown in figure 5.2.

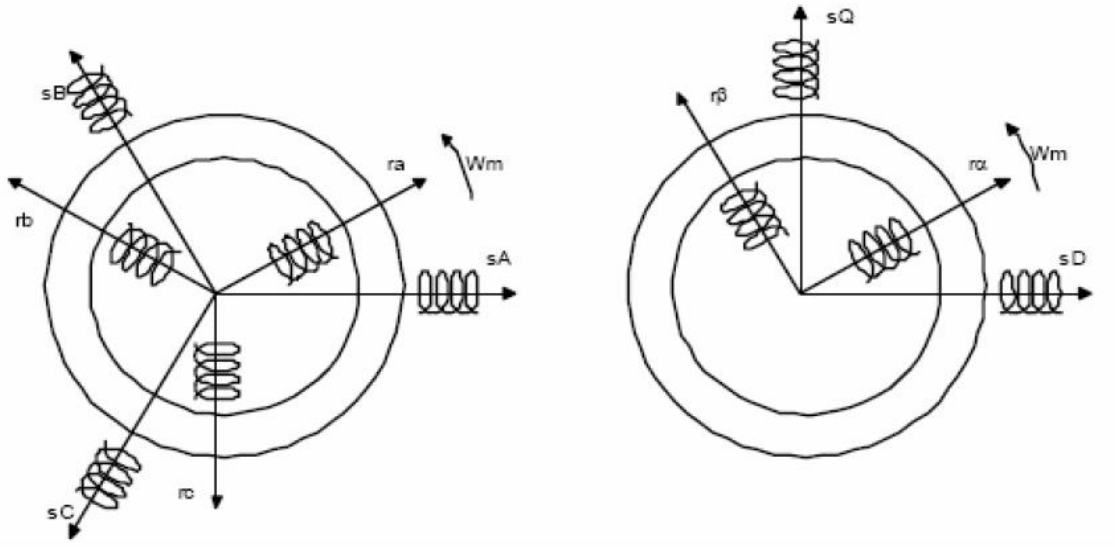

Figure 5.2: equivalent axis transformation

In this model, the direct and the quadrature-axis stator magnitudes are imaginary. The relationship between the 2-axis voltages and the 3-axis voltages are given by the following transformation:

$$\begin{bmatrix} V_{sD} \\ V_{sQ} \\ V_{s0} \end{bmatrix} = c.\begin{bmatrix} \cos\theta & \cos(\theta-2\pi/3) & \cos(\theta+2\pi/3) \\ -\sin\theta & -\sin(\theta-2\pi/3) & -\sin(\theta+2\pi/3) \\ 1/\sqrt{2} & 1/\sqrt{2} & 1/\sqrt{2} \end{bmatrix}.\begin{bmatrix} V_{sA} \\ V_{sB} \\ V_{sC} \end{bmatrix} \quad (5.10)$$

$$\begin{bmatrix} V_{sA} \\ V_{sB} \\ V_{sC} \end{bmatrix} = c.\begin{bmatrix} \cos\theta & -\sin\theta & 1/\sqrt{2} \\ \cos(\theta-2\pi/3) & -\sin(\theta-2\pi/3) & 1/\sqrt{2} \\ \cos(\theta+2\pi/3) & -\sin(\theta+2\pi/3) & 1/\sqrt{2} \end{bmatrix}.\begin{bmatrix} V_{sD} \\ V_{sQ} \\ V_{s0} \end{bmatrix} \quad (5.11)$$

Here "c" is a constant and takes values 2/3 or 1. These previous equations are applicable for magnitudes of other variables such as currents and fluxes too.

Simplification of equation 5.9 by applying the mentioned Park's transform.

$$\begin{bmatrix} V_{sD} \\ V_{sQ} \\ V_{r\alpha} \\ V_{r\beta} \end{bmatrix} = \begin{bmatrix} R_s+pL_s & -L_s p\theta_s & pL_m & -L_m(P\omega_m+p\theta_r) \\ L_s p\theta_s & R_s+pL_s & L_m(P\omega_m+p\theta_r) & pL_m \\ pL_m & -L_m(-P\omega_m+p\theta_s) & R_r+pL_r & -L_r p\theta_r \\ L_m(-P\omega_m+p\theta_s) & pL_m & L_r p\theta_r & R_r+pL_r \end{bmatrix}.\begin{bmatrix} i_{sD} \\ i_{sQ} \\ i_{r\alpha} \\ i_{r\beta} \end{bmatrix} \quad (5.12)$$

where $L_s = L_s - L_m$; $L_r = L_r - L_m$; $L_m = \frac{3}{2}\bar{M}_{sr}$ (5.13)

5.1.4. Voltage matrix equations:

On simplifying expression 5.12, we obtain new matrixes as shown below:

5.1.4.1. Fixed to the stator: Then $\omega s = 0$ and hence $\omega_r = (-)\omega_m$

$$\begin{bmatrix} V_{sD} \\ V_{sQ} \\ V_{rD} \\ V_{rQ} \end{bmatrix} = \begin{bmatrix} R_s+pL_s & 0 & pL_m & 0 \\ 0 & R_s+pL_s & 0 & pL_m \\ pL_m & L_m(P\omega_m) & R_r+pL_r & L_r(P\omega_m) \\ L_m(-P\omega_m) & pL_m & -L_r(P\omega_m) & R_r+pL_r \end{bmatrix}.\begin{bmatrix} i_{sD} \\ i_{sQ} \\ i_{rD} \\ i_{rQ} \end{bmatrix} \quad (5.14)$$

5.1.4.2. Fixed to the rotor: Then $\omega_r = 0$ and consequently $\omega_s = \omega_m$

$$\begin{bmatrix} V_{sD} \\ V_{sQ} \\ V_{rD} \\ V_{rQ} \end{bmatrix} = \begin{bmatrix} R_s + pL_s & -L_s(P\omega_m) & pL_m & -L_m(P\omega_m + p\theta_r) \\ L_s(P\omega_m) & R_s + pL_s & L_m(P\omega_m + p\theta_r) & pL_m \\ pL_m & 0 & R_r + pL_r & 0 \\ 0 & pL_m & 0 & R_r + pL_r \end{bmatrix} \cdot \begin{bmatrix} i_{sD} \\ i_{sQ} \\ i_{rD} \\ i_{rQ} \end{bmatrix} \quad (5.15)$$

5.1.4.3 – Fixed to the synchronism: Then $\omega_r = s \cdot \omega_s$.

$$\begin{bmatrix} V_{sD} \\ V_{sQ} \\ V_{rD} \\ V_{rQ} \end{bmatrix} = \begin{bmatrix} R_s + pL_s & -L_s\omega_s & pL_m & -L_m(P\omega_m + p\theta_r) \\ L_s\omega_s & R_s + pL_s & L_m(P\omega_s) & pL_m \\ pL_m & -L_m(\omega_s) & R_r + pL_r & -L_r(\omega_s) \\ L_m(\omega_s) & pL_m & L_r(\omega_s) & R_r + pL_r \end{bmatrix} \cdot \begin{bmatrix} i_{sD} \\ i_{sQ} \\ i_{rD} \\ i_{rQ} \end{bmatrix} \quad (5.16)$$

5.2. SPACE PHASOR NOTATION

5.2.1. Introduction

Space phasor notation helps in transforming the natural instantaneous three phase system onto a complex plane on the rotor cross section. In that plane, the space phasor rotates at the angular frequency of the three phase system. A space phasor rotating with a similar angular speed, as an example, will describe the rotating field of force. In case of steady state, i.e. the supply voltages being sinusoidal and symmetrical; the space phasor become equal to three-phase voltage phasors, allowing complex analysis possibilities. The 120º operator is used to transform the induction motor model in its natural coordinates to its space phasor form.

$$\mathbf{a} = e^{j2\pi/3}; \mathbf{a}^2 = e^{j4\pi/3} \quad (5.17)$$

Thus, the current stator space phasor is:

$$\bar{i}_s = c.\left[1.i_{sA}(t) + a.i_{sB}(t) + a^2.i_{sC}(t)\right] \quad (5.18)$$

Here "c" is a constant and takes values 2/3 or 1. These previous equations are applicable for magnitudes of other variables such as currents and fluxes too.

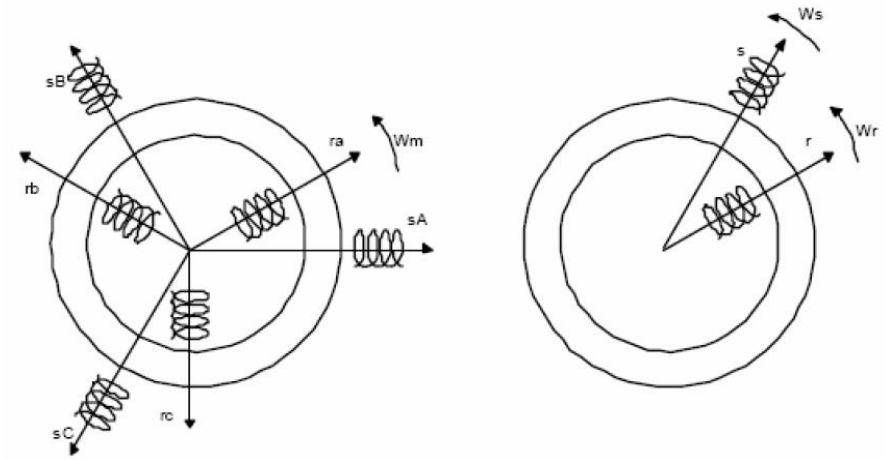

Figure 5.3: Space phasor representation of three phase quantities

5.2.2. Current space phasors.

In this section, the Induction machine's assumptions as in section 3.1.1 are further analyzed. It is represented in figure 3.4 the model of the induction machine in two different frames, the stationary frame i.e. the **D-Q** axis, assumed fixed to the stator, and the rotating frame i.e. the α-β axis fixed to the rotor.

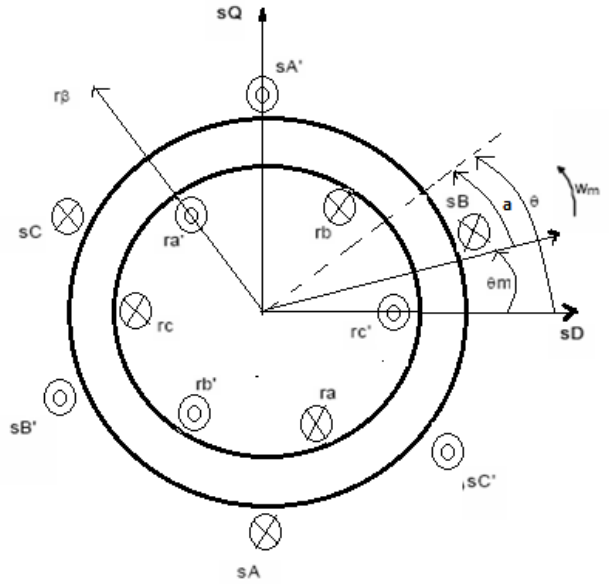

Fig 5.4.Cross-section model of the induction machine in two different frames, the stationary frame, i.e. the **D-Q** axis, assumed fixed to the stator, and the rotating frame i.e. the α-β axis fixed to the rotor.

The stator current space phasor can be expressed as follows:

$$\bar{i}_s = \frac{2}{3}\left[i_{sA}(t) + a.i_{sB}(t) + a^2 i_{sC}(t) \right] = \left|\bar{i}_s\right| e^{j\theta} \qquad (5.19)$$

Expressed in the reference frame fixed to the stator, here **sD** is the real–axis representation and **sQ** is the imaginary axis representation.

The equivalence between the stator phasor and the D-Q two-axis components is:

$$\bar{i}_s = i_{sD}(t) + j.i_{sQ}(t) \qquad (5.20)$$

Or:

$$\mathrm{Re}(\bar{i}_s) = \mathrm{Re}\left[\frac{2}{3}\left(i_{sA} + a.i_{sB} + a^2 i_{sC}\right)\right] = i_{sD} \qquad \text{--------- (5.21)}$$

$$Im(\bar{i}_s) = \mathrm{Im}\left[\frac{2}{3}\left(i_{sA} + a.i_{sB} + a^2 i_{sC}\right)\right] = i_{sQ} \qquad \text{--------- (5.22)}$$

The association between the real stator phase currents and the space phasor current can be conveyed as follows:

$$\mathrm{Re}(\bar{i}_s) = \mathrm{Re}\left[\frac{2}{3}\left(i_{sA} + a.i_{sB} + a^2 i_{sC}\right)\right] = i_{sA} \quad \text{--------- (5.23)}$$

$$\mathrm{Re}(\bar{i}_s) = \mathrm{Re}\left[\frac{2}{3}\left(a^2.i_{sA} + i_{sB} + a.i_{sC}\right)\right] = i_{sB} \quad \text{--------- (5.24)}$$

$$\mathrm{Re}(\bar{i}_s) = \mathrm{Re}\left[\frac{2}{3}\left(a.i_{sA} + a^2.i_{sB} + i_{sC}\right)\right] = i_{sC} \quad \text{--------- (5.25)}$$

In a analogous way, the rotor current in space phasor form is as follows:

$$\bar{i}_r = \frac{2}{3}\left[i_{ra}(t) + a.i_{rb}(t) + a^2 i_{rc}(t)\right] = \left|\bar{i}_r\right| e^{j\alpha} \quad \text{--------- (5.26)}$$

Here rα represents the real axis of the reference frame fixed to rotor while rβ represents the corresponding imaginary axis.

Hence the new reference frame space phasor of the rotor current becomes:

$$\bar{i}_r' = \left|\bar{i}_r\right| e^{j\theta} = \left|\bar{i}_r\right| e^{j(\alpha+\theta_m)} \quad \text{- -------- (5.27)}$$

The similarity between the current rotor space phasor and the α-β two-axis is as follows:

$$\bar{i}_r = i_{r\alpha(t)} + j.i_{r\beta}(t) \quad \text{--------- (5.28)}$$

Or:

$$\mathrm{Re}(\bar{i}_r) = \mathrm{Re}\left[\frac{2}{3}\left(i_{ra} + a.i_{rb} + a^2 i_{rc}\right)\right] = i_{r\alpha} \quad \text{--------- (5.29)}$$

$$\mathrm{Im}(\bar{i}_r) = \mathrm{Im}\left[\frac{2}{3}\left(i_{ra} + a.i_{rb} + a^2 i_{rc}\right)\right] = i_{r\beta} \quad \text{--------- (5.30)}$$

The correlation between the space phasor current and the real stator currents are expressed as follows:

$$\mathrm{Re}(\bar{i}_r) = \mathrm{Re}\left[\frac{2}{3}\left(i_{ra} + a.i_{rb} + a^2 i_{rc}\right)\right] = i_{ra} \quad \text{--------- (5.31)}$$

$$\mathrm{Re}(a^2\bar{i}_r) = \mathrm{Re}\left[\frac{2}{3}\left(a^2 i_{ra} + i_{rb} + a.i_{rc}\right)\right] = i_{rb} \quad \text{--------- (5.32)}$$

$$\mathrm{Re}(a\bar{i}_r) = \mathrm{Re}\left[\frac{2}{3}\left(a.i_{ra} + a^2.i_{rb} + i_{rc}\right)\right] = i_{rc} \quad \text{--------- (5.33)}$$

In the stationary reference frame, the space phasor of magnetizing current becomes :

$$\overline{i_m} = \overline{i_s} + \left(N_{re} / N_{se} \right) \overline{i_r'} \qquad \text{--------- (5.34)}$$

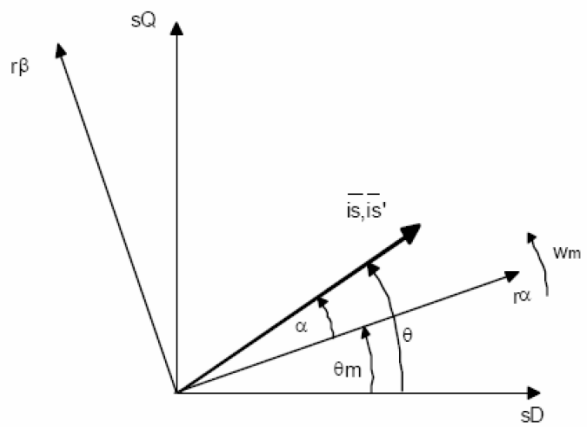

Fig 5.5. Stator-current space phasor communicated as per the rotational frame altered to the rotor and the stationary frame settled to the stator.

5.3. Torque Expressions

5.3.1. Introduction

Torque can be generally expressed as follows:

$$T = c. \overline{\psi_s} \times \acute{i}_r \qquad (5.35)$$

Where the c is a constant, space phasor of stator flux is ψ_s and space phasor for rotor current being $\acute{i}_r$ both referred to the stationary frame of reference on stator.

In another expression, it follows:

$$T = c.|\overline{\psi_s}|.|\acute{i}_r| \sin\gamma \qquad (5.36)$$

Where Υ is the angle existing between the stator flux linkage and the rotor current.

It takes after that when $\gamma = 90^o$ the torque got is the most extreme and its interpretation is precisely equivalent to the one for the DC machines. All things considered, in DC machines the space dispersion of both sizes is altered in space, hence transforming the most extreme torque for all diverse size qualities. Besides, both extents might be controlled freely or independently. In an AC machine, in any case, it is considerably more troublesome to understand this standard in light of the fact that both amounts are coupled and their position in space relies on upon both the stator and rotor positions. It is a further complexity that in squirrel-cage machines, it is not conceivable to screen the rotor current, unless the engine is uniquely ready for this reason in an exceptional lab.

5.3.2. Deduction of the torque expression by means of energy considerations.

Conservation of energy is considered to derive the essential torque equation. Hence our starting equation is:

$P_{mechanical} = P_{electric} - P_{loss} - P_{field}$

Substituting the previous powers for its values, the equation can be expressed as follows:

$$T.\omega_r = \frac{3}{2}\left[\left(Re(\bar{V}_s.\bar{i}_s^*) - R_s|i_s|^2 - Re(\frac{d\psi_s}{dt}\bar{i}_s^*)\right) + \left(Re(\bar{V}_r.\bar{i}_r^*) - R_r|i_r|^2 - Re(\frac{d\psi_r}{dt}\bar{i}_r^*)\right)\right] \quad (5.37)$$

Subsequently as in the stationary reference frame, the stator ohmic loss in the stator and the rate of change of stator flux linkage control the final value of the stator voltage space phasor $\bar{V}_s$, the above expressions can be transformed to:

$$T.\omega_r = \frac{3}{2} Re(-j\omega_r\bar{\psi_r}\bar{i_r}) = -\frac{3}{2}\omega_r Re(\bar{\psi_r}\bar{i_r}) = -\frac{3}{2}\omega_r\bar{\psi_r} \times \bar{i_r} \quad (5.38)$$

Expressing the equation in a general way for any number of pair of poles gives, and substituting further, different expressions for the torque can be obtained as follows:

$$T = \frac{3}{2}\omega_r\bar{\psi_r} \times \bar{i_r} \quad (5.39)$$

$$T = \frac{3}{2}\omega_r\bar{\psi_s} \times \bar{i_s} \quad (5.40)$$

5.3.3. Torque constant

$$T = \frac{3}{2} P (\psi_{sD} . i_{sQ} - \psi_{sQ} . i_{sD}) \quad (5.41)$$

The torque constant 'c' can take two particular values as denoted by the following table. The constants used in the phasor diagram affect which value is being chosen. Both possibilities are shown in table 5.1.

	Non Power Invariant		Power Invariant	
Torque constant	**3/2**		**1**	
	3 → 2	**2 → 3**	**3 → 2**	**2 → 3**
Space phasor constant	2/3	1	$\sqrt{(2/3)}$	$\sqrt{(2/3)}$

Table 5.1 Torque constant values

'3→2' represents the transformation from three axis to either two axis or space phasor notation and '2→3' represents the vice versa.

5.4. Simulink Model

5.4.1. Equations used in the model

The last declarations utilized as a part of the actualized models are gotten from all the formerly presented representations. All mathematical statements have been re-masterminded keeping in mind the end goal to utilize the operator 1/s rather than the operator p because MATLAB "Simulink" handles the integrator better than derivative.

5.4.1.1. Stator Reference

Stator and rotor fluxes can be expressed as follows:

$$\psi_{sD} = \frac{1}{s}\left(V_{sD} - R_s i_{sD}\right)$$

$$\psi_{sQ} = \frac{1}{s}\left(V_{sQ} - R_s i_{sQ}\right)$$

$$\psi_{rD} = \frac{1}{s}\left(-R_r i_{rD} - P.\omega_m \psi_{rq}\right)$$

$$\psi_{rQ} = \frac{1}{s}\left(-R_r i_{rQ} + P.\omega_m \psi_{rd}\right) \quad (5.42)$$

Stator and rotor currents can be expressed as follows:

$$i_{sD} = \psi_{sD}\frac{L_r}{L_x} - \psi_{rd}\frac{L_m}{L_x}$$

$$i_{sD} = \psi_{sD}\frac{L_r}{L_x} - \psi_{rd}\frac{L_m}{L_x}$$

$$i_{rd} = \psi_{rd}\frac{L_s}{L_x} - \psi_{sD}\frac{L_m}{L_x}$$

$$i_{rq} = \psi_{rq}\frac{L_s}{L_x} - \psi_{sQ}\frac{L_m}{L_x} \quad (5.43)$$

Where $L_x = L_s L_r - L_m^2$

5.4.1.2. Motion equation

The motion equation is as follows:

$$T - T_L = J\frac{d\,\omega_m}{dt} + D\omega_m \quad (5.44)$$

Here T represents the developed electromagnetic torque and T_L the load torque. J represents rotor's inertia, and D stands for damping constant.

Using the torque expressions 5.44, the previous motion equation can be expressed as follows:

$$P.c.\left(\psi_{sD} i_{sQ} - \psi_{sQ} i_{sD}\right) = T_L + \omega_m(D + Js)$$

$$\omega_r = \frac{P.c.\left(\psi_{sD} i_{sQ} - \psi_{sQ} i_{sD}\right) - T_L}{D+Js} \quad (5.45)$$

Here P is the number of pair of poles and the torque constant takes the values of 1 or 2/3 according to the table 5.1.

The SIMULINK model for induction motor is developed by using above equations and simulated successfully. The SIMULINK model is given in figure 5.6 and induction motor sub block model also presented in figure 5.7. The wave forms of stator current in stationary and rotating reference frames and induction motor torque and speed waveforms given in figures.

A selection of one of three common reference frames is obtained by clicking the manual switches:

a) Stator frame where wk=0 and thetak=0 indicated in cyan color.

b) Synchronous frame where wk=ws and thetak = wo int(ws) indicated in red.

c) Rotor frame where wk=wm and thetak = wo int(wm) in green.

Both upper and lower pair of switches must be in the same up or down positions. The induction machine modeling is done so as to conform to the state vector model. The parameters describing the electromechanical system are expressed in per unit. There is control over the amplitude as well as frequency of the A.C excitation. This simulation considers the system at stand by setting all the opening conditions to zero.

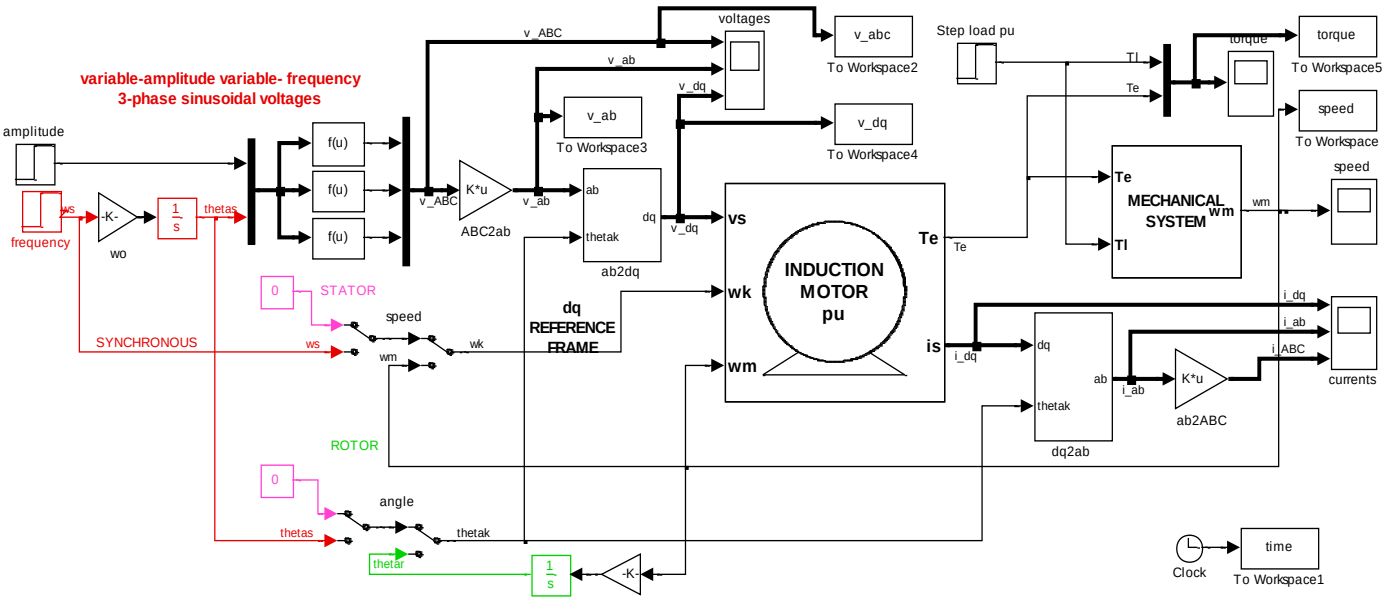

Figure 5.6: SIMULINK model for Induction motor to obtain voltages and currents in different frames of references

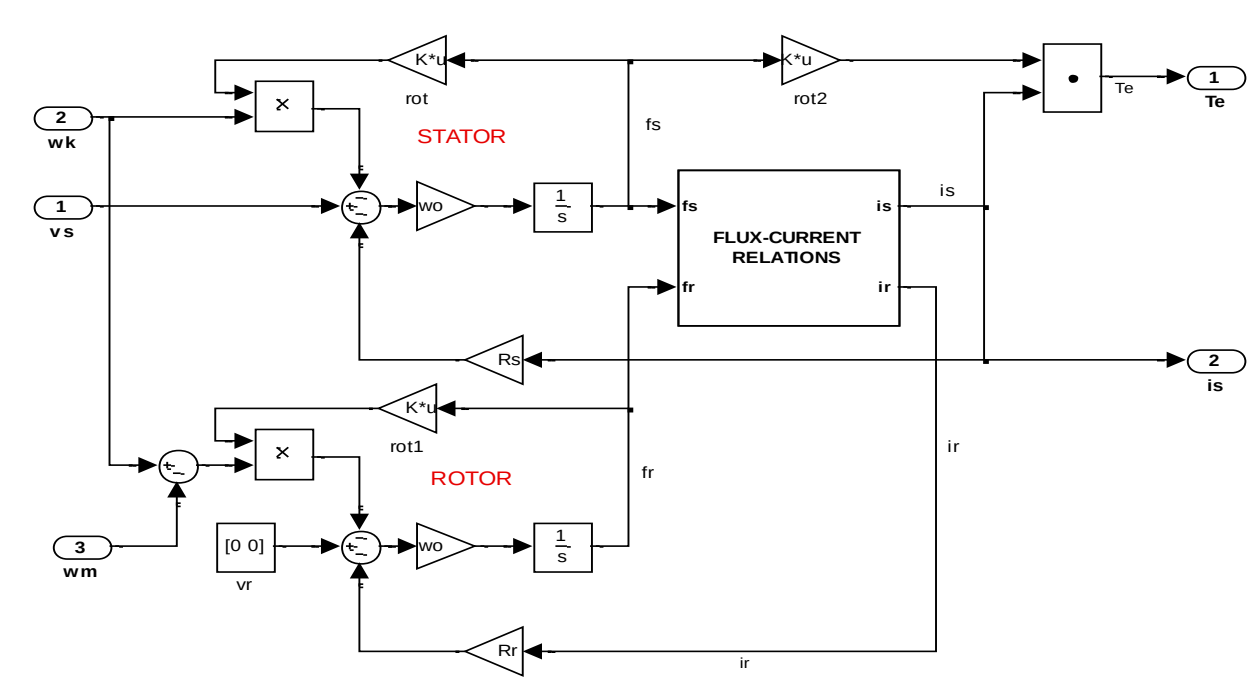

Figure 5.7: Vectorized Dynamic Model of the induction machine in arbitrary reference frame

wo is the base frequency 2*pi*fo [rad/s] where fo = 50 Hz

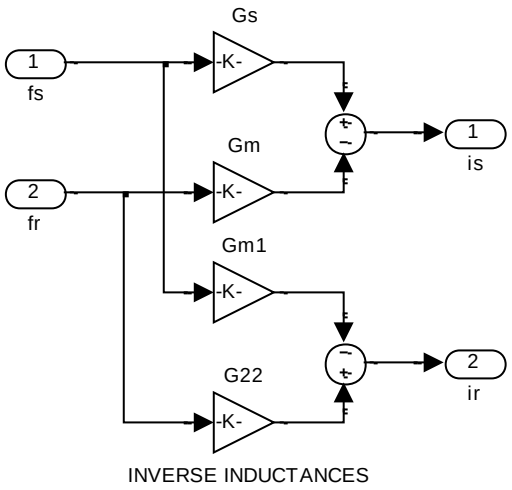

Fig. 5.8. Flux Current Relations block

The starting of the motor is done at voltage and frequency magnitudes at the rated values; without any loading. The full load is applied in the form of a step function as soon as the steady state is reached.

The waveforms of the currents and voltages can be observed and are plotted in both stator and rotating frame. It should be noted that, in steady-state, the stator currents and voltages rotate at stator frequency w_s in the stator frame, as dc quantities in the synchronous frame, and at slip frequency (w_s-w_m) in the rotor frame. The following waveforms obtained from the simulation demonstrate the above observations:

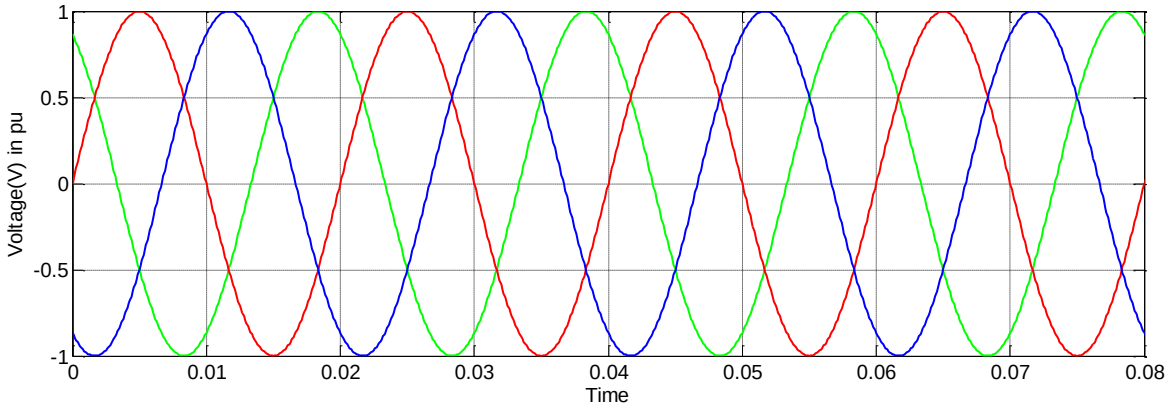

Fig. 5.9. 3-ϕ supply voltage

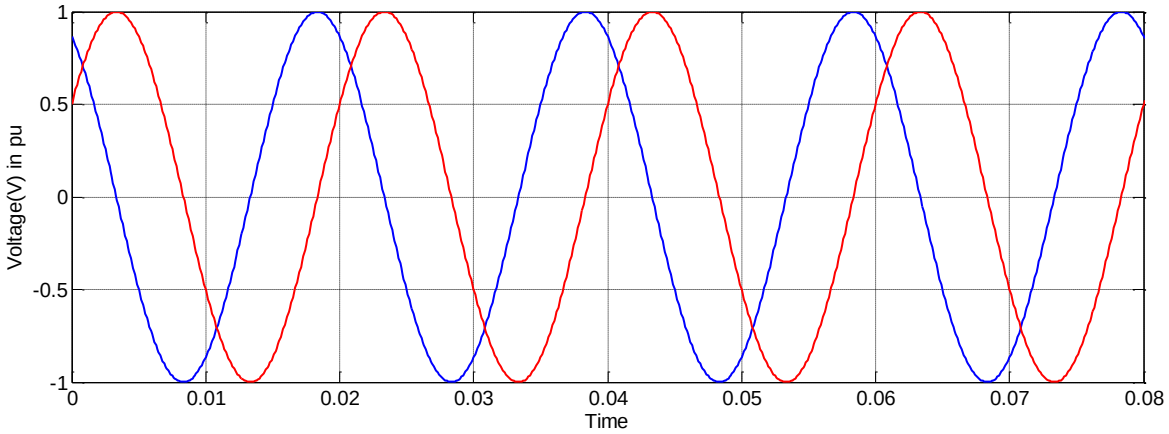

Fig. 5.10. Induction motor stator voltages in stationary reference frame

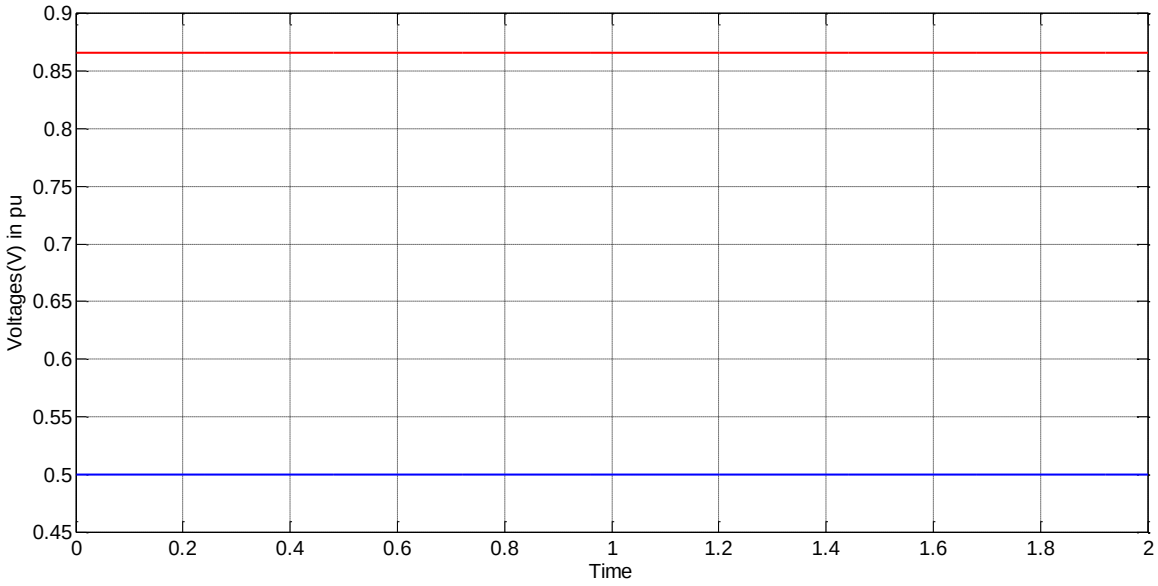

Fig. 5.11. Induction motor stator voltages in synchronously rotating frame

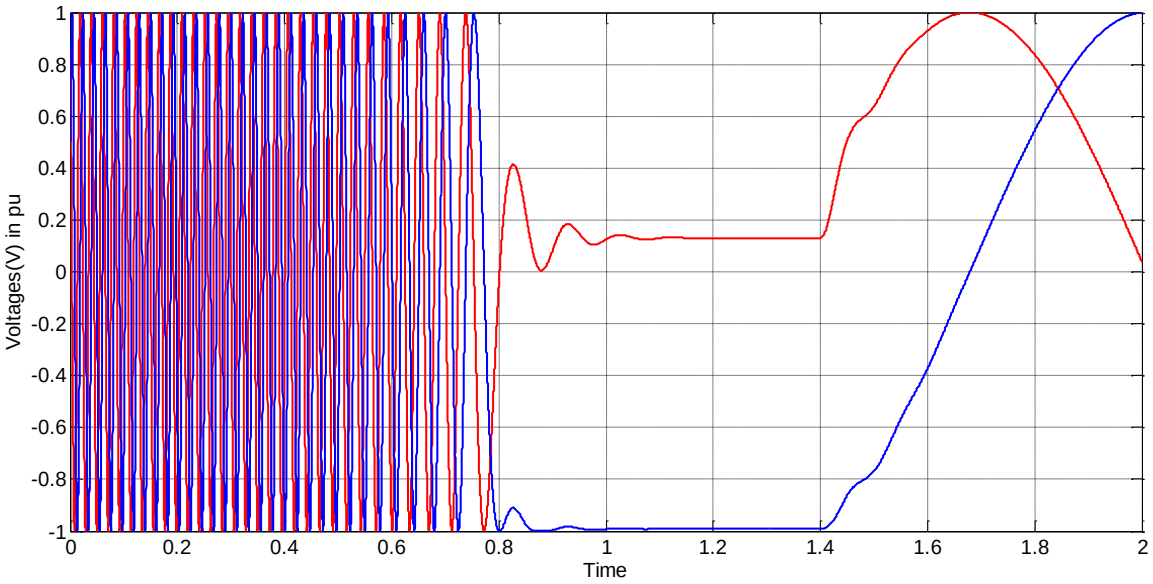

Fig. 5.12. Induction motor stator voltages in rotor reference frame

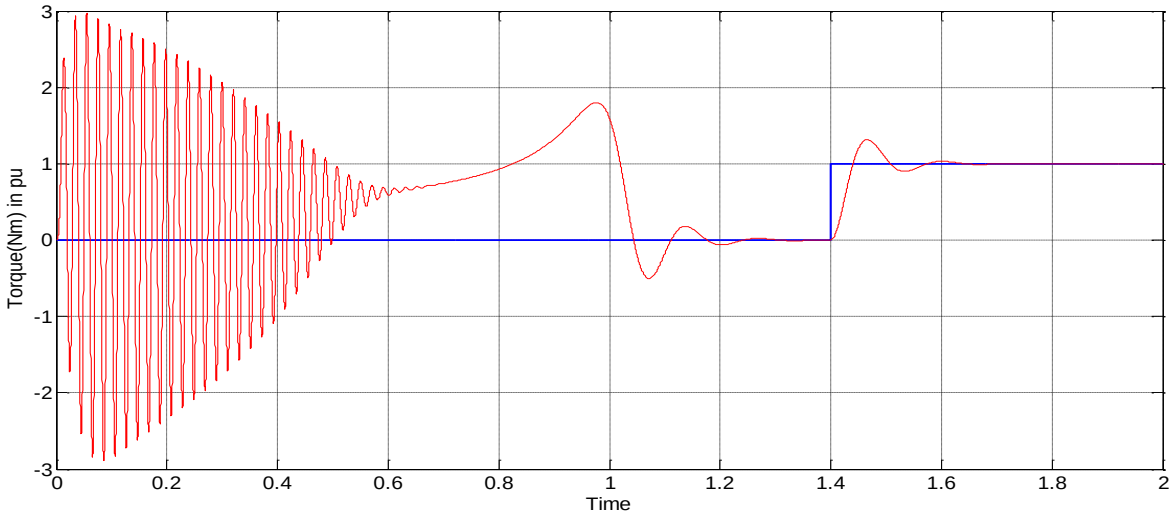

Fig. 5.13. Torque output of induction motor

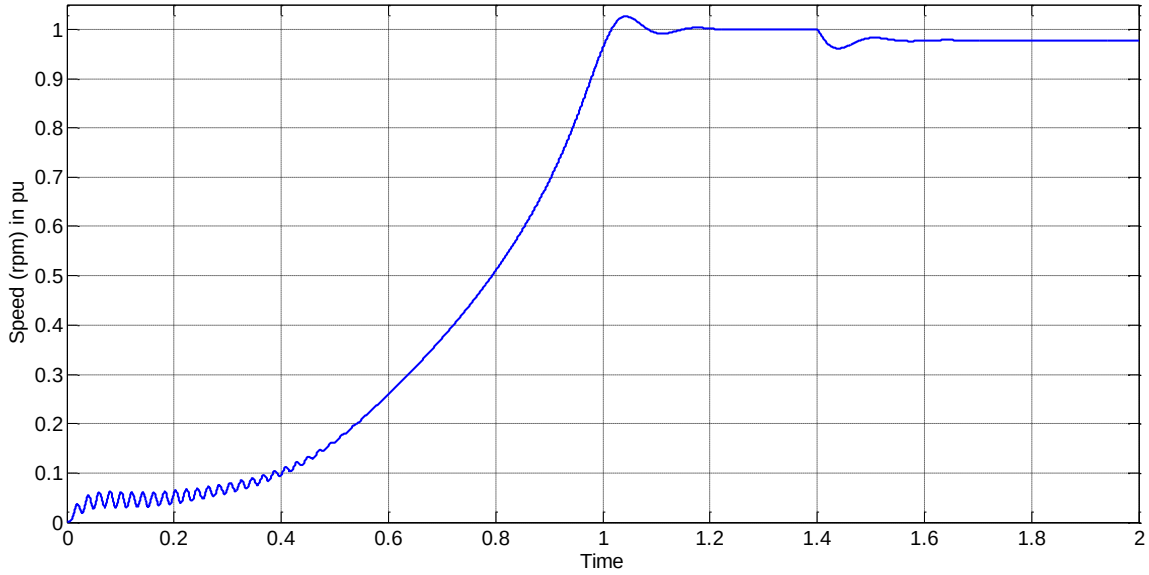

Fig. 5.14. Speed of the induction motor

5.5. DETAILS OF SIMULATION FIGURES AND RESULTS

The magnitude of the gains rot, rot1 and rot 2 are $\begin{bmatrix} 0 & -1 \\ 1 & 0 \end{bmatrix}$

The magnitude of the gain Gs = $\frac{Lrl + Lm}{(Lsl * Lrl) + (Lsl * Lm) + (Lrl * Lm)}$

The magnitude of the gain Gm = $\frac{Lm}{(Lsl * Lrl) + (Lsl * Lm) + (Lrl * Lm)}$

Similarly the magnitude of the gain Gm1 = $\frac{Lm}{(Lsl * Lrl) + (Lsl * Lm) + (Lrl * Lm)}$

And magnitude of gain G22 = $\frac{Lsl + Lm}{(Lsl * Lrl) + (Lsl * Lm) + (Lrl * Lm)}$

5.6 INTERIM CONCLUSIONS:

In the present chapter we have deduced the motor model. The model has been formulated by means of the two-axis theory equations and the space phasor notation. Despite the fact that both nomenclatures are valid, it has been proved that the space phasor notation is much more compact and easier to work with. The model has been developed in both nomenclatures for the stator, rotor and synchronous references. In further chapters, the motor model with stator reference, introduced in section 3.4.1.1, will be the one most used. The final concrete equations used in the MATLAB/SIMULINK motor model have been presented by the three different references. Some simulations are shown to prove the validity of the model, being equal for the previously mentioned three references. Finally the steady state motor analysis has been introduced.

CHAPTER 6

DIRECT TORQUE CONTROL OF INDUCTION MOTOR

6.1 Introduction

6.2 DTC controller

6.3 DTC schematic

6.4 SIMULINK Model

6.5 Interim Conclusions

6.1 INTRODUCTION:

6.1.1 DC drive analogy:

In a dc machine, neglecting the armature reaction effect and field saturation, the developed torque is given by

$$T = K_a \, . \, I_a \, . \, I_f \tag{6.1}$$

where I_a is the armature current and I_f is the field current.

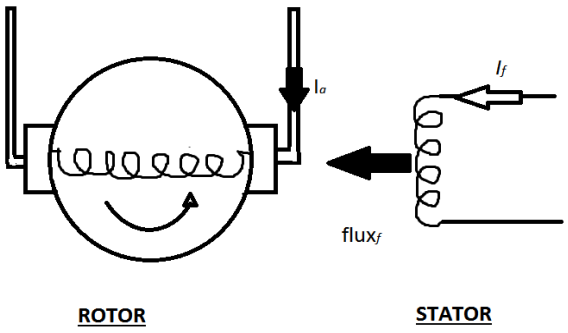

Figure 6.1 DC motor model

We know in DC motor current I_f produces field flux ψ_f and I_a, current that flows through the armature produces armature flux ψ_a. DC machine is constructed in such a way that ψ_f is always orthogonal to ψ_a. By nature the flux vectors are fixed in space, perpendicular to each other and decoupled from each other. Hence, ψ_f remains unchanged when we change the torque by means of armature current. The other benefits are for rated ψ_f we obtain high torque/A ratio and speedy transient response.

Direct Torque Controlled (DTC) drives permits to attain the performance similar to DC motor. DTC drives decouple torque and flux components from each other with the help of hysteresis loop. The physical real-time and predicted values of torque and flux are compared in the hysteresis loop. DTC controller, torque and flux predictor and voltage-source inverter (VSI) are the main components of DTC drives.

6.1.2 Principle of direct torque control of induction motor:

An induction motor is powered by a VSI in a DTC drive. DTC chooses the optimum inverter voltage vector, hence leads to directly change stator flux ψ_s and torque. The flux and torque errors are limited within individual hysteresis limits by appropriate choice inverter voltage vector. Hence both torque response and efficiency are at the peak every time. DTC also reduces losses in harmonics, acoustic noise and transient response.

The developed electromagnetic torque of induction motor can be written as:

$$T = \frac{3}{2} P \overline{\psi_s} \times \overline{i_s}$$

where the quantity of pole pairs is given by P, stationary reference frame stator flux is denoted by ψ_s and stator current by i_s. By revising the equation, it can be written as:

$$T = \frac{3}{2} P |\overline{\psi_s}||\overline{i_s}| \sin(\alpha_s - \rho_s)$$

where angle of the stator flux is denoted by ρ_s and that of the current by α_s. The angles are measured in reference to horizontal axis of stationary reference frame fixed. By keeping the magnitude of stator flux unchanged and just changing angle ρ_s rapidly, we can directly change the developed torque.

We can yield similar result by applying another expression which can be expressed as:

$$T = \frac{3}{2} P \frac{L_m}{L_s L_r - L_m^2} |\overline{\psi_r}||\overline{\psi_s}| \sin(\rho_s - \rho_r)$$

Since rotor time constant is more than stator time constant, the stator flux varies quickly over rotor flux. So rotor flux is presumed constant. Hence if we maintain stator flux modulus unchanged, then we can control developed torque just by varying the angle $\rho_s - \rho_r$.

6.2 - DTC CONTROLLER:

We can select the optimum VSI state to implement the needed stator flux. By neglecting ohmic drops for uncomplicatedness, stator flux depends on the stator voltage according to the following equations:

$$\frac{d\,\overline{\psi_s}}{dt} = \overline{V_s}$$

Or:

$$\Delta\overline{\psi_s} = \overline{V_s} \cdot \Delta t$$

By controlling radial and tangential components of stator flux space vector in its locus, we can attain decoupled nature of stator flux modulus and torque. The components of identical voltage space vector in similar directions determine the former two components. Hence, in DTC drive it is vital to select the optimum voltage vector from the exact voltage source inverter state.

6.2.1 Voltage Source Inverter

Many configurations of voltage source inverter, possessing high possible output voltage vectors are used in DTC drive. The most widely used is the six pulse inverter. The six pulse inverter supplies the IM with variable

frequency AC voltage. The inverter can be supplied either from a DC source like battery, or rectifier, powered from AC source.

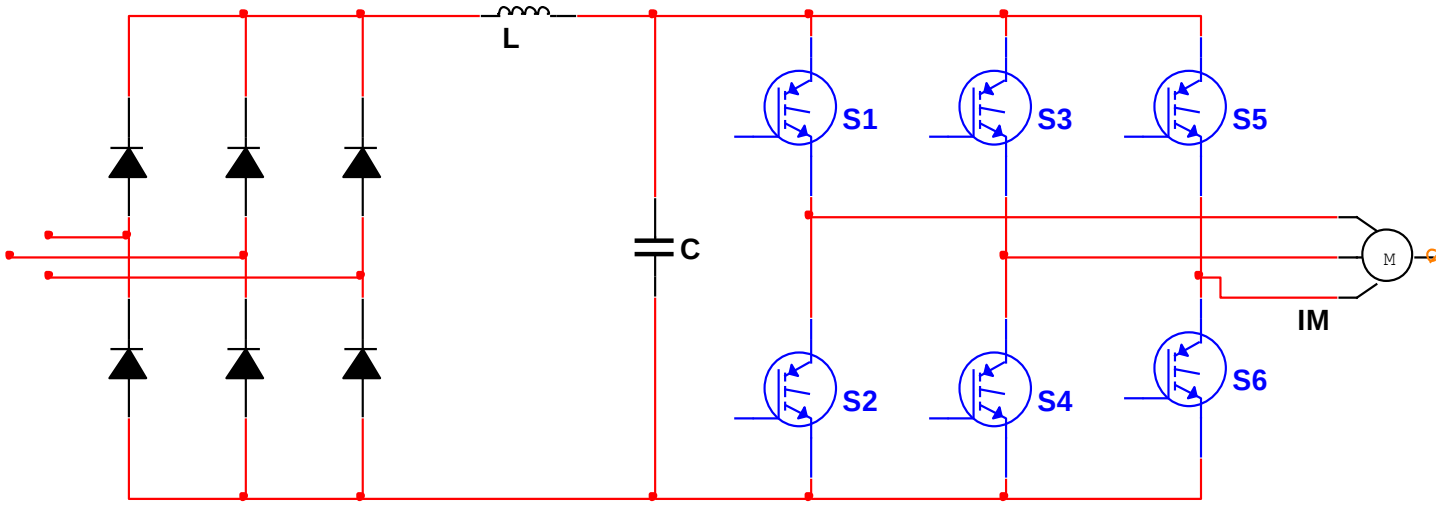

Figure 6.2: Voltage source inverter

The function of inductor is to keep the fault currents within limits. The function of the large electrolytic capacitor C is to smooth DC link voltage.

The VSI bridge should be made of switches proficient of turned off and on. Hence, Insulated Gate Bipolar Transistors (IGBTs) are employed. An anti-parallel diode is connected across each IGBT to allow motor current to flow after the IGBT is turned off.

Each leg of the inverter has two switches. One of the switch is attached to positive side of DC link, while the other to the negative side. We have to make sure that at any time, only one of the two switches can be switched on. We allocate binary number 1 to a leg if the positive switch of the leg is ON and number 0 if the negative switch is ON. Hence, looking at groupings of mode of each leg, we discover that the inverter has eight switching modes (VaVbVc = 000-111). V0 (000) and V7 (111) are the zero voltage vectors because the ends of motor are shorted. V1 to V6 are the nonzero voltage vectors.

Now evaluating the inverter switching modes using the DQ transformation equations for the stationary reference frame we attain stationary reference DQ model of VSI. We observe that six nonzero voltage vectors will be oriented as depicted in the following diagram. The diagram also depicts the likely dynamic locus of stator flux, and the changes of the flux with switching of the inverter states. We separate the entire locus into six different sectors which are depicted by the dashed lines.

We observe that the stator flux is attained directly from inverter voltage. By selecting the optimum VSI state we can attain the needed locus of stator flux locus. Hence, magnitude and position of stator voltage vector determine the direction and speed of the stator flux locus in space.

For the torque to be increased, we need to select the voltage vector that will spread the flux vector towards the way of rotation. For the torque to be decreased, we need to select a zero switching vector. Summing up, when

stator flux vector is in s-th sector with motor running in counter-clockwise direction, then to increase the torque, we need to select Vs+1 or Vs+2 stator voltage vectors. To decrease the torque we need to select zero voltage

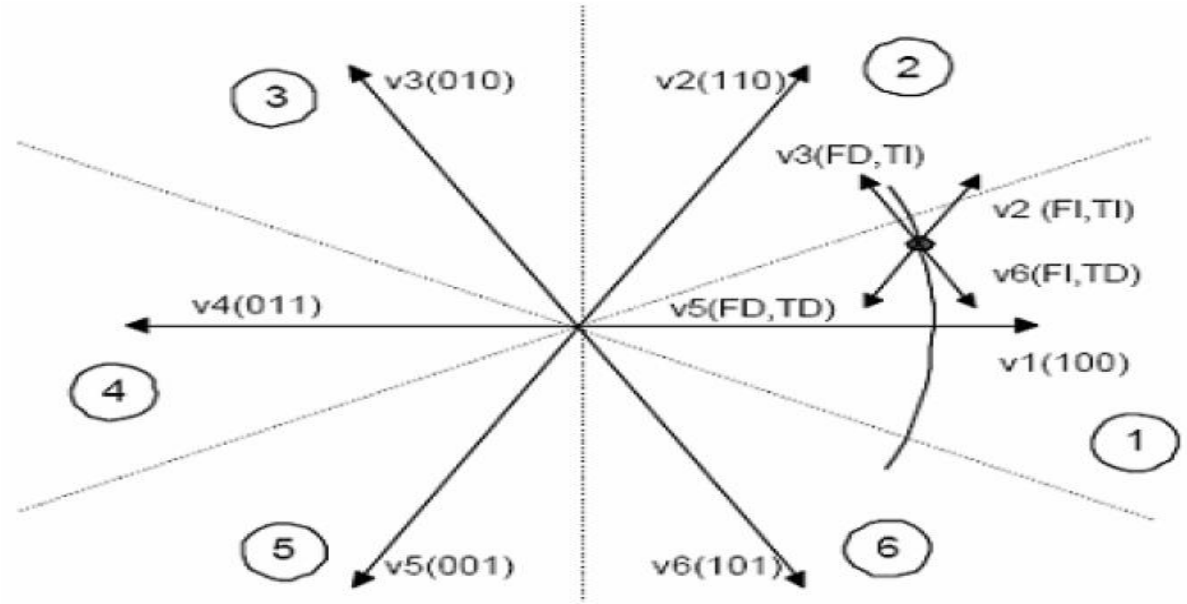

Figure 6.3: Stator flux vector locus and different possible switching; Voltage vectors. FD: flux decrease. FI: flux increase. TD: torque decrease. TI: torque increase

vector V0 or V7. Overall, to increase modulus of stator flux, when stator flux vector is in s-th sector, we use switching vectors Vs-1 for clockwise rotation or Vs+1 for counter-clockwise rotation, and to decrease the magnitude, we apply voltage vectors Vs-2 for clockwise rotation or Vs+2 for counter-clockwise rotation.

VOLTAGE VECTOR	INCREASE	DECREASE
Stator Flux	V_s, V_{s+1}, V_s-1	$V_{s+2}, V_{s-2}, V_{s+3}$
Torque	V_{s+1}, V_{s+2}	V_{s-1}, V_{s-2}

Table 6.1: General Selection Table for Direct Torque Control, "s" denotes the sector number.

Flux Error $d\psi$	Torque Error dT	S1	S2	S3	S4	S5	S6
1	1	V_2	V_3	V_4	V_5	V_6	V1
	0	V_0	V_7	V_0	V_7	V_0	V_7
	-1	V_6	Vi	V_2	V_3	V_4	V_5
0	1	V_3	V_4	V_5	V_6	V1	V_2
	0	V_0	V_7	V_0	V_7	V_0	V_7
	-1	V_5	V_6	V1	V_2	V_3	V_4

Table 6.2: DTC look-up table

6.3 DTC SCHEMATIC:

From the schematic of DTC drive, we observe that we use two separate loops analogous to magnitude of stator flux and torque. The physical real-time values of stator flux magnitude and torque are matched with the reference values and resultant values are input to the corresponding hysteresis blocks. We feed the lookup table with the yields of respective hysteresis loops and position of stator flux. Hence, we are able to limit the errors in stator flux magnitude and torque inside the boundaries. Plan of DTC verifies, for appropriate choice of voltage sector from lookup table, the drive requires predictions of stator flux and torque.

6.3.1 Methods for Estimation of Stator Flux in DTC:

In DTC drives, in order to guarantee suitable operation and stability, we need to predict the flux accurately. Flux prediction methods proposed are built on voltage model, current model, or amalgamation of both. The present DTC structure uses a voltage model to predict flux and torque, without the application of a shaft encoder and using stator resistance as the only parameter.

$$\psi_{sD} = \int (V_{sD} - R_s I_{sD}) dt = i_{sD} . \frac{L_x}{L_m} + \psi'_{rD} . \frac{L_m}{L_r}$$

$$\psi_{sQ} = \int (V_{sQ} - R_s I_{sQ}) dt = i_{sQ} . \frac{L_x}{L_m} + \psi'_{rQ} . \frac{L_m}{L_r}$$

And we can predict the torque by the expression:

$$T = \frac{3}{2} P (\psi_{sD} . i_{sQ} - \psi_{sQ} . i_{sD})$$

After predicting the values from above model we continue to lookup table to choice the appropriate voltage vector.

6.4 SIMULINK MODEL FOR CONVENTIONAL DTC:

We design the SIMULINK model of DTC drive of IM employing IM model offered previous chapter and also develop a MATLAB program to execute orthodox DTC drive. We develop and simulate the SIMULINK model of the orthodox DTC drive. The waveform for induction motor torque, which is obtained from simulation of MATLAB program is presented and verified with the SIMULINK waveforms.

A three dimensional matrix is developed by MATLAB program which is applied by the SIMULINK model and is given as under:

```
%switching table for DTC
clc,clear
a(:,:,1) =[1 0 2;5 7 6];
a(:,:,2) =[5 7 3;4 0 2];
a(:,:,3) =[4 0 1;6 7 3];
a(:,:,4) =[6 7 5;2 0 1];
```

a(:,:,5) =[2 0 4;3 7 5];

a(:,:,6) =[3 7 6;1 0 4];

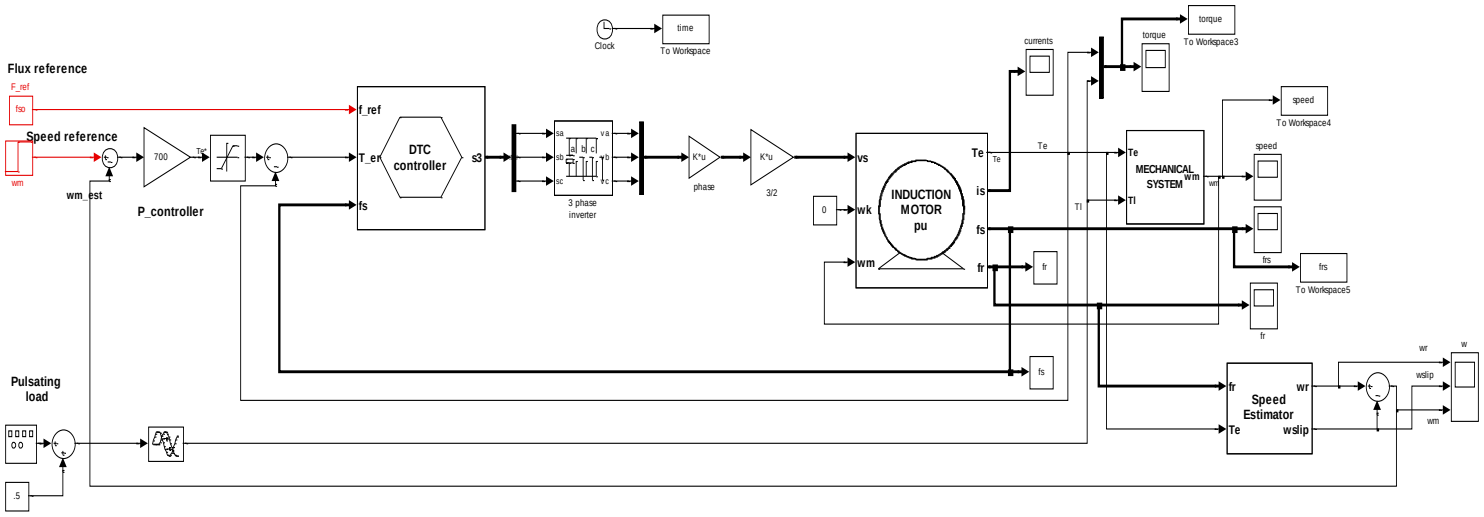

Figure 6.4: DTC of induction motor

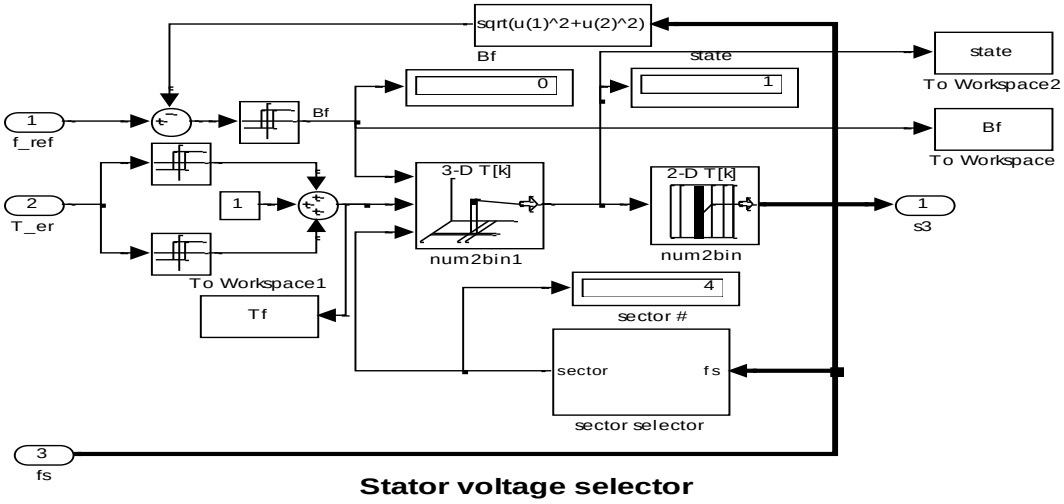

Figure 6.5: SIMULINK model for conventional DTC

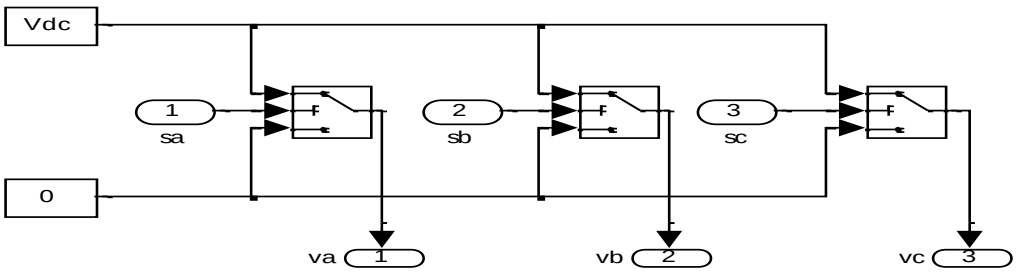

Figure 6.6: SIMULINK model of voltage source inverter

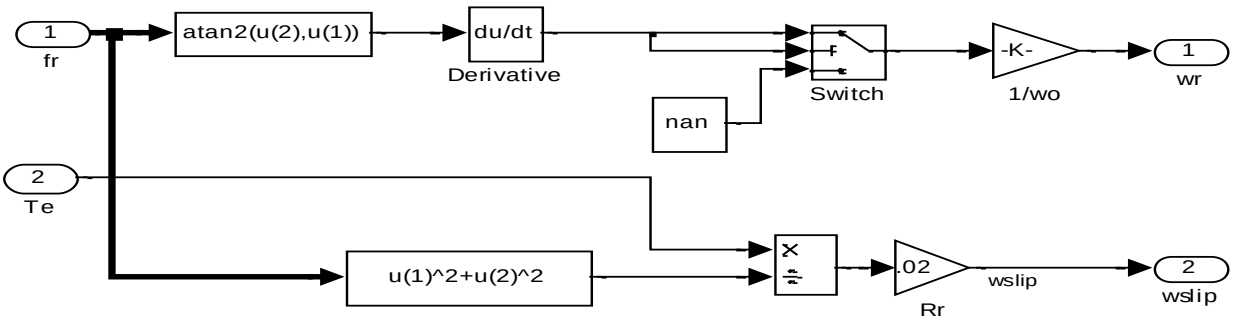

Figure 6.7: SIMULINK model of speed estimator

The waveform for torque of the induction motor with the application of pulsating load torque of 1N.m with speed reference of 0.8pu, is given in figure 4.8, which is obtained from simulation of MATLAB program with a sampling time of 0.0002. It indirectly means that the drive output is updated at a rate of 5 KHz.

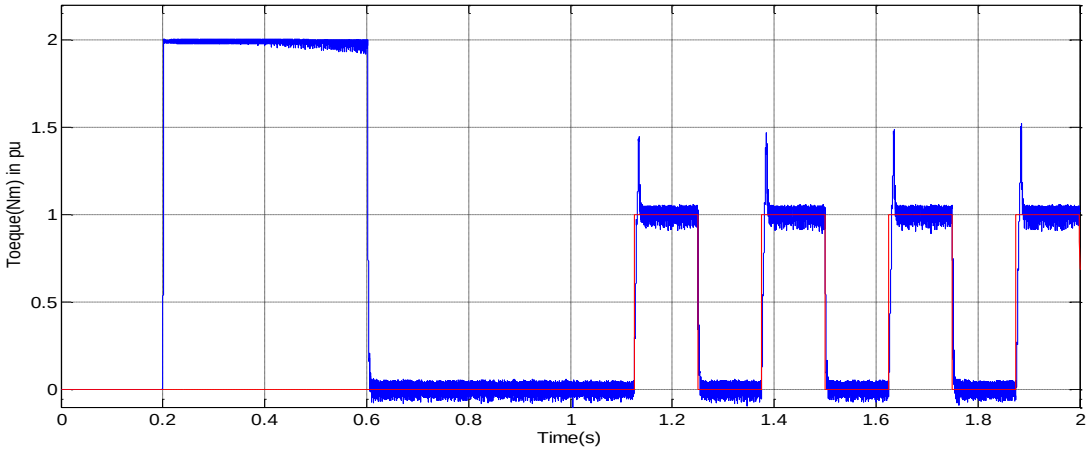

Figure 6.8: Torque output of induction motor

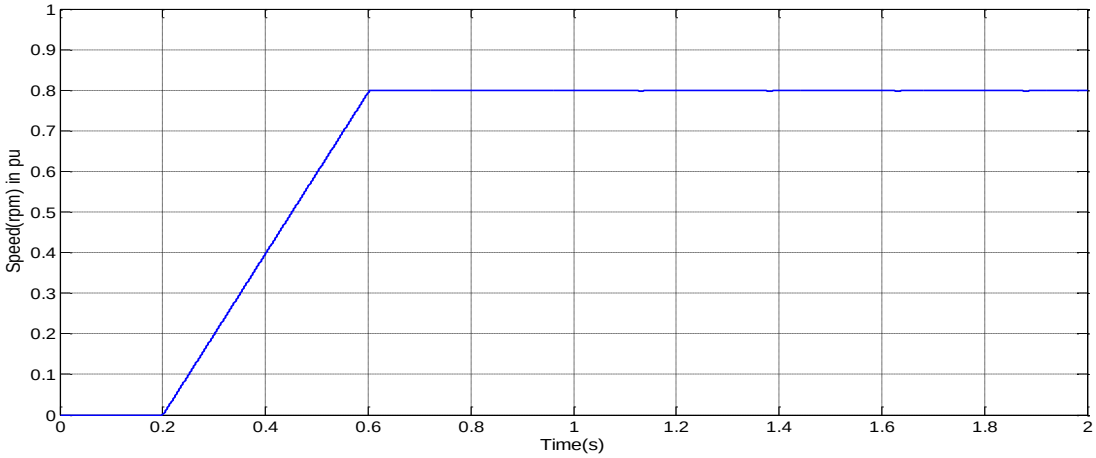

Fig. 6.9. Speed output of induction motor

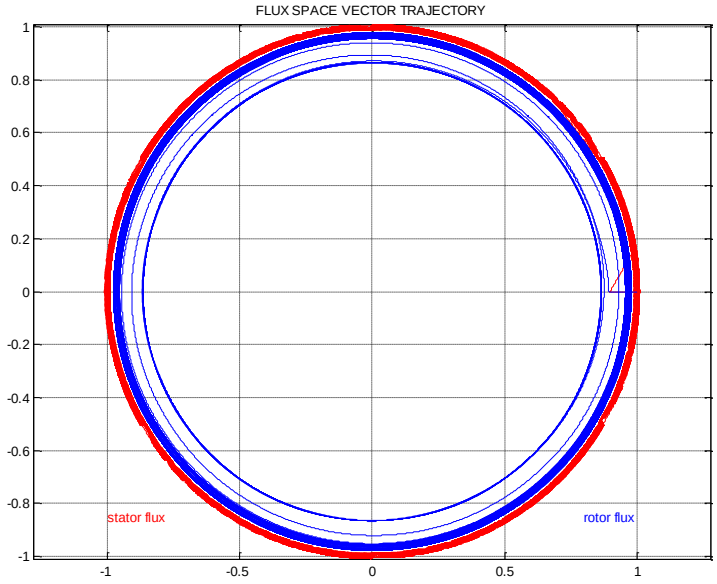

Figure 6.10: Flux space vector trajectory of stator and rotor flux

6.5 INTERIM CONCLUSIONS:

From the torque waveform obtained from simulation of conventional DTC, it is cleared that the torque ripple is 0.6 Nm (approximately 1.8-1.2 Nm maximum and minimum values respectively) with the conventional DTC. This high magnitude of torque ripple is the main drawback of conventional DTC. The other drawbacks also summarized as follows:

- The system is not being able to separate big and small errors in flux and torque are not distinguished. It uses similar vectors throughout start up, step changes and also during steady state.
- It demonstrates slow reaction while starting and during variations in either flux or torque.

CONCLUSION

In order to overcome the mentioned drawbacks, there are different solutions, like space vector modulation based DTC, non-artificial intelligence methods, mainly "sophisticated tables" and fuzzy logic based systems.

In this project we have analyzed the concept of direct torque control (DTC) – Direct Speed Control (DSC) for the induction motor in a concise and systematic manner. The idea of the DTC-DSC procedure for IM has been broke down by method for physical contemplations, systematic advancements, simulations and test outcomes, showing how the stator flux amplitude and the motor torque could be held under control through the requisition of the voltage space vectors produced by a VSI.

As in any sensor less IM drive, the execution of a DTC drive crumbles at low speed. On the other hand, it has been outlined that the utilization of an enhanced flux estimator gives the drive great execution even in those working conditions. A few changes to essential DTC plan have been examined and a feasible answer for flux debilitating operation has been exhibited.

For driving any induction motor, the DTC has been realized to be the best controller in the market at present. This new control technique's principles are being extensively studied and its applications are being exhaustively realized. In this thesis, we have also made it a point to demonstrate the decoupling control of motor torque and motor stator flux as introduced by the DTC.

SIMULINK/MATALB® model has been fully developed. From the results it is apparent that DTC strategy provides us with an implementation-al advantage over the other vector controls because of its independence from co-ordinate transformers and voltage modulators. One of the major drawbacks of this control scheme may be the introduction of ripples in the final torque estimates, which is very detrimental to the induction machines.

7.2 Future work:

All future work is summarized schematically in the following ideas:

- Developments of space vector modulation based DTC to reduce the torque ripple.
- The developed controller must be self-adaptive.
- The controller must be able to provide satisfactory results for any machine specifications.
- It should produce less noise and distortion in the final waveforms..
- Study the torque ripple reduction with multilevel converters.
- Sensor less space vector modulation based DTC implementation, just sensing two currents and the DC voltage.

APPENDICES

Appendix 1: MATLAB Code for Speed Control of 3-ϕ Induction motor using Variable Rotor Resistance

```
function out = inductionvarRr()
Vl1 = input('Enter the Suppy Voltage (line to line) RMS value: ');
P = input('Enter the number of poles: ');
Rs = input('Stator Resistance: ');
Rr1 = input('Enter the first Rotor Resistance: ');
Rr2 = input('Enter the second Rotor Resistance: ');
Rr3 = input('Enter the third Rotor Resistance: ');
Rr4 = input('Enter the fourth Rotor Resistance: ');
Rr5 = input('Enter the fifth Rotor Resistance: ');
Xs = input('Stator Leakage Reactance @ 50 Hz frequecny: ');
Xr = input('Rotor Leakage Reactance @ 50 Hz frequecny: ');

Ls=Xs/(2*pi*50);
Lr=Xr/(2*pi*50);

Wsync1=4*pi*50/P;

Tmf1=zeros(Wsync1*500+1,1);
Tmf2=zeros(Wsync1*500+1,1);
Tmf3=zeros(Wsync1*500+1,1);
Tmf4=zeros(Wsync1*500+1,1);
Tmf5=zeros(Wsync1*500+1,1);

m=1;    for Wrotor1=0:0.002:Wsync1

    Tmf1(m)=(3*(((Vl1^2)*Rr1/((Wsync1-Wrotor1)/Wsync1))/((Rs+Rr1/((Wsync1-
Wrotor1)/Wsync1))^2+(2*pi*50*Ls+2*pi*50*Lr)^2))/Wsync1); %star connected
    m=m+1;
end
m=1;   for Wrotor1=0:0.002:Wsync1

    Tmf2(m)=(3*(((Vl1^2)*Rr2/((Wsync1-Wrotor1)/Wsync1))/((Rs+Rr2/((Wsync1-
Wrotor1)/Wsync1))^2+(2*pi*50*Ls+2*pi*50*Lr)^2))/Wsync1);
    m=m+1;
end
m=1;   for Wrotor1=0:0.002:Wsync1

    Tmf3(m)=(3*(((Vl1^2)*Rr3/((Wsync1-Wrotor1)/Wsync1))/((Rs+Rr3/((Wsync1-
Wrotor1)/Wsync1))^2+(2*pi*50*Ls+2*pi*50*Lr)^2))/Wsync1);
    m=m+1;
end
m=1;   for Wrotor1=0:0.002:Wsync1

    Tmf4(m)=(3*(((Vl1^2)*Rr4/((Wsync1-Wrotor1)/Wsync1))/((Rs+Rr4/((Wsync1-
Wrotor1)/Wsync1))^2+(2*pi*50*Ls+2*pi*50*Lr)^2))/Wsync1);
    m=m+1;
end
m=1;   for Wrotor1=0:0.002:Wsync1

    Tmf5(m)=(3*(((Vl1^2)*Rr5/((Wsync1-Wrotor1)/Wsync1))/((Rs+Rr5/((Wsync1-
Wrotor1)/Wsync1))^2+(2*pi*50*Ls+2*pi*50*Lr)^2))/Wsync1);
    m=m+1;
end

plot(Tmf1); hold on; plot(Tmf2); plot(Tmf3); plot(Tmf4); plot(Tmf5); hold off;
ylabel('Torque(N-m)'); xlabel('Rotor Speed(Rad/s)'); end
```

Appendix 2: MATLAB Code for Speed Control of 3-ϕ Induction motor using Variable Stator Voltage

```
function out = inductionvarV()
Vl1=input('Enter the first Suppy Voltage (line to line) RMS value: ');
Vl2=input('Enter the second Suppy Voltage (line to line) RMS value: ');
Vl3=input('Enter the third Suppy Voltage (line to line) RMS value: ');
Vl4=input('Enter the fourth Suppy Voltage (line to line) RMS value: ');
Vl5=input('Enter the fifth Suppy Voltage (line to line) RMS value: ');
P=input('Enter the number of poles: ');
Rs=input('Stator Resistance: ');
Rr=input('Rotor Resistance: ');
Xs=input('Stator Leakage Reactance @ 50 Hz frequecny: ');
Xr=input('Rotor Leakage Reactance @ 50 Hz frequecny: ');

Ls=Xs/(2*pi*50);
Lr=Xr/(2*pi*50);

Wsync1=4*pi*50/P;

Tmf1=zeros(Wsync1*500+1,1);
Tmf2=zeros(Wsync1*500+1,1);
Tmf3=zeros(Wsync1*500+1,1);
Tmf4=zeros(Wsync1*500+1,1);
Tmf5=zeros(Wsync1*500+1,1);

m=1;    for Wrotor1=0:0.002:Wsync1

    Tmf1(m)=(3*(((Vl1^2)*Rr/((Wsync1-Wrotor1)/Wsync1))/((Rs+Rr/((Wsync1-
Wrotor1)/Wsync1))^2+(2*pi*50*Ls+2*pi*50*Lr)^2))/Wsync1); %star connected
    m=m+1;
end

m=1;   for Wrotor1=0:0.002:Wsync1

    Tmf2(m)=(3*(((Vl2^2)*Rr/((Wsync1-Wrotor1)/Wsync1))/((Rs+Rr/((Wsync1-
Wrotor1)/Wsync1))^2+(2*pi*50*Ls+2*pi*50*Lr)^2))/Wsync1);
    m=m+1;
end

m=1;   for Wrotor1=0:0.002:Wsync1

    Tmf3(m)=(3*(((Vl3^2)*Rr/((Wsync1-Wrotor1)/Wsync1))/((Rs+Rr/((Wsync1-
Wrotor1)/Wsync1))^2+(2*pi*50*Ls+2*pi*50*Lr)^2))/Wsync1);
    m=m+1;
end

m=1;   for Wrotor1=0:0.002:Wsync1     Tmf4(m)=(3*(((Vl4^2)*Rr/((Wsync1-
Wrotor1)/Wsync1))/((Rs+Rr/((Wsync1-
Wrotor1)/Wsync1))^2+(2*pi*50*Ls+2*pi*50*Lr)^2))/Wsync1);
    m=m+1;
end

m=1;   for Wrotor1=0:0.002:Wsync1

    Tmf5(m)=(3*(((Vl5^2)*Rr/((Wsync1-Wrotor1)/Wsync1))/((Rs+Rr/((Wsync1-
Wrotor1)/Wsync1))^2+(2*pi*50*Ls+2*pi*50*Lr)^2))/Wsync1);
    m=m+1;
end
plot(Tmf1); hold on; plot(Tmf2); plot(Tmf3); plot(Tmf4); plot(Tmf5); hold off;
ylabel('Torque(N-m)'); xlabel('Rotor Speed(Rad/s)'); end
```

Appendix 3: MATLAB Code for Speed Control of 3-ϕ Induction motor using Constant V/f control

```
function out = inductionconstVf()
Vll=input('Suppy Voltage (line to line) RMS value @ 50 Hz: '); f2=input('Enter the
second frequency: '); f3=input('Enter the third frequency: '); f4=input('Enter the
fourth frequency: '); f5=input('Enter the fifth frequency: ');
P=input('Enter the number of poles: ');
Rs=input('Stator Resistance: ');
Rr=input('Rotor Resistance: ');
Xs=input('Stator Leakage Reactance @ 50 Hz frequecny: ');
Xr=input('Rotor Leakage Reactance @ 50 Hz frequecny: ');

Ls=Xs/(2*pi*50);
Lr=Xr/(2*pi*50);

Vlnf1=Vll/(3^0.5);
Vlnf2=Vlnf1*f2/50;
Vlnf3=Vlnf1*f3/50;
Vlnf4=Vlnf1*f4/50; Vlnf5=Vlnf1*f5/50;

Wsync1=4*pi*50/P;
Wsync2=4*pi*f2/P;
Wsync3=4*pi*f3/P;
Wsync4=4*pi*f4/P;
Wsync5=4*pi*f5/P;

Tmf1=zeros(Wsync1*500+1,1);
Tmf2=zeros(Wsync2*500+1,1);
Tmf3=zeros(Wsync3*500+1,1);
Tmf4=zeros(Wsync4*500+1,1);
Tmf5=zeros(Wsync5*500+1,1);
  m=1;    for Wrotor1=0:0.002:Wsync1

    Tmf1(m)=(3*(((Vlnf1^2)*Rr/((Wsync1-Wrotor1)/Wsync1))/((Rs+Rr/((Wsync1-
Wrotor1)/Wsync1))^2+(2*pi*50*Ls+2*pi*50*Lr)^2))/Wsync1); %star connected
    m=m+1;
  end

  m=1;   for Wrotor2=0:0.002:Wsync2

    Tmf2(m)=(3*(((Vlnf2^2)*Rr/((Wsync2-Wrotor2)/Wsync2))/((Rs+Rr/((Wsync2-
Wrotor2)/Wsync2))^2+(2*pi*f2*Ls+2*pi*f2*Lr)^2))/Wsync2);
    m=m+1;
  end

  m=1;  for Wrotor3=0:0.002:Wsync3

    Tmf3(m)=(3*(((Vlnf3^2)*Rr/((Wsync3-Wrotor3)/Wsync3))/((Rs+Rr/((Wsync3-
Wrotor3)/Wsync3))^2+(2*pi*f3*Ls+2*pi*f3*Lr)^2))/Wsync3);
    m=m+1;
  end

  m=1;   for Wrotor4=0:0.002:Wsync4

    Tmf4(m)=(3*(((Vlnf4^2)*Rr/((Wsync4-Wrotor4)/Wsync4))/((Rs+Rr/((Wsync4-
Wrotor4)/Wsync4))^2+(2*pi*f4*Ls+2*pi*f4*Lr)^2))/Wsync4);
    m=m+1;
  end

  m=1;   for Wrotor5=0:0.002:Wsync5
```

```
 Tmf5(m)=(3*(((Vlnf5^2)*Rr/((Wsync5-Wrotor5)/Wsync5))/((Rs+Rr/((Wsync5-
Wrotor5)/Wsync5))^2+(2*pi*f5*Ls+2*pi*f5*Lr)^2))/Wsync5);
    m=m+1;
  end

  plot(Tmf1); hold on; plot(Tmf2); plot(Tmf3); plot(Tmf4); plot(Tmf5); hold off;
ylabel('Torque(N-m)'); xlabel('Rotor Speed(Rad/s) * 100'); end
```

REFERENCES:

[1] Takahashi, I. and Noguchi, T. "A new quick-response and high efficiency control Strategy of an induction motor." IEEE Transactions on Industry Applications, vol.22, no. 5, pp. 820-827, 1986.

[2] Novotny, D. W. and Lipo, T. A. “Vector Control and Dynamics of AC Drives.” Oxford University Press Inc, New York, 1996.

[3] Vas, P. "Sensor less Vector and Direct Torque Control". Oxford University Press 1998.

[4] Bose, B. K.; "Power Electronics and AC Drives". Prentice-Hall. 1986.

[5] Mohan, Undeland, Robbins. “Power Electronics". Wiley. Second edition. 1989.

[6] Ludtke, I.; Jayne M.G. “A comparative study of high performance speed control strategies for voltage sourced PWM inverter fed induction motor drives”, Seventh International Conference on electrical Machines and Drives, 11-13 September 1995, University of Durham, UK.

[7] Tamai, S., Sugimoto, H. and Yano, M. "Speed sensorless vector control of induction motor with model reference adaptive system." IEEE Industrial Applications Society Annual Meeting, Atlanta, pp.189-195, 1987.

[8] Schauder, C. "Adaptive speed identification for vector control of induction motors without rotational transducers." IEEE Transactions on Industrial Applications, vol.28, pp. 1054-1061, 1992.

[9] Doki, S., Sangwongwanich, S. and Okuma, S. "Implementation of speed sensorless field oriented vector control using adaptive sliding observer." IEEE-IECON, San Diego, pp. 453-458, 1992.

[10] Kawamura, A. and Hoft, R. "An analysis of induction motor for field oriented or vector control." IEEE Power Electronics Specialists Conference, Albuquerque, New Mexico, pp. 91-100, 1983.

[11] Kubota, H. and Matsuse, K. "Speed sensorless field oriented control of induction machines." IEEE IECON, Bologna, Italy, pp. 1611-1615, 1994.

[12] Mir, S. and Elbuluk, M. "Precision torque control in inverter fed induction machines using fuzzy logic". Conf. Rec. IEEE-PESC Annual Meeting, Atlanta, pp. 396-401, 1995.

[13] Depenbrock, M. "Direct self control (DSC) of inverter–fed induction machine." IEEE Transactions on Power Electronics, vol. 3, no. 4, pp. 420-429, 1988.

[14] Mir, S. and Elbuluk, M. "Precision torque control in inverter fed induction machines using fuzzy logic." Conf. Rec. IEEE-PESC Annual Meeting, Atlanta, pp. 396-401, 1995.

[15] Thomas, G., Halbetler, H. and Deepakraj, M. D. "Control strategies for direct torque control using discrete pulse modulation." IEEE Transactions on Industry Applications, vol. 27, pp. 893-901, 1991.

[16] Takahashi, I and Ohimori, Y. “High-Performance Direct Torque Control of an Induction Motor”, IEEE Trans. Industry Applications, Vol. 25, pages 257-264, March 1989.

[17] Perelmuter, V. "Three level inverters with direct torque control.” IEEE Proc. on Industry Applications, pp. 1368-1373, 2000.